

UNIVERSITY OF TWENTE.

**Faculty of Engineering
Technology (CTW)**

Optimization and redesign of actuators for a medical device

Noor (E.M.J.) Ooms
Internship report at DEMCON
May 2016

Supervisors:

Dr.Ir. D. van de Belt (UTWENTE)

Dr. Ir. D. Tjepkema (DEMCON)

Department Biomechanical Engineering
University of Twente
P.O. Box 217
7500 AE Enschede
The Netherlands

Abstract

Demcon is developing custom designed actuators for a medical company which are used in a therapeutic vest worn by patients who suffer from cystic fibrosis. The actuators create oscillating forces in a predetermined force profile on the patient's thorax that helps to loosen the mucus in the lungs. This can be coughed up at a later stage. The current design of the actuator has magnets to create force with the current through the coil, and leaf springs that cause pretension and linear guidance of the back iron.

A sensitivity analysis on the influence of variations in the actuator parameters on the therapy force is performed. These actuator parameters are: mass of the moveable body, stiffness of the springs that are used to connect the moveable body to the static part of the actuator, coil resistance, coil inductance, and the (position dependent) motor constant. This sensitivity analysis is done using simulations in Matlab/Simulink, and analytically using the Taylor series expansion. The Matlab/Simulink model is optimised and the tolerances of the parameters are determined. Results were used to optimise and improve the control system of the actuator. This decreased the dissipated power and improved the accuracy of the applied therapy force.

After that, a redesign of the actuator is made in order to lower weight. A therapeutic vest contains eight actuators of 550 grams each, which makes the vest very heavy. The main goal of the redesign is to lower weight to 350 grams per actuator and keep the other functionalities of the actuator the same. The redesign contains a ball bearing which causes linear guidance of the back iron, and helical compression springs to generate the pretension of the back iron. The new actuator is easy to assemble and has a minimum amount of components. Furthermore, the actuator is 15% smaller in volume and weighs only 331 grams.

Keywords: Demcon, cystic fibrosis, voice coil actuator, sensitivity analysis, design of an actuator

Table of Content

Introduction	6
Chapter 1: Analysis of the actuator	7
1.1. Mechanical design of the actuator	7
1.2. Actuator requirements.....	7
1.3. Therapy force waveform generation	8
1.4. Engineering formulas for actuator optimisation	8
1.5. The model	9
1.6. Matlab/Simulink model	10
Chapter 2: Sensitivity analysis.....	12
2.1. Discretisation problem.....	12
2.1.1. Solution 1: Higher sample frequency	13
2.1.2. Solution 2: Correction factor based on function fit	14
2.1.3. Solution 3: Correction factor based on a look-up table.....	14
2.1.4. Solution selection.....	14
2.2. Sensitivity analysis.....	15
2.3. Analytical solution.....	17
Chapter 3: Waveform optimisation	19
3.1. Testing new waveforms.....	19
3.2. Optimising original waveform.....	20
Chapter 4: Verifying the assumed rigid thorax	22
Chapter 5: Redesign of the actuator	24
5.1. Reduction of the motor parameters and therapy parameters	24
5.2. Functional design in FEMM.....	25
5.3. Morphological diagram.....	27
5.3.1. Pretension	28
5.3.2. Linear guidance.....	31
5.3.3. Elimination	34
5.4. Concepts.....	34
5.4.1. Concept 1: compression-extension springs with ball bearing	34
5.4.2. Concept 2: compression springs with ball bearing	36
5.4.3. Concept 3: compression springs with elastic bearing.....	37
5.4.4. Concept 4: membrane spring.....	38
5.4.5. Summary of the concepts	39
5.5. Selection of the concepts.....	39
5.6. Final concept.....	40
5.6.1. Total overview	40

5.6.2.	Optimization and adjustments.....	41
5.6.3.	Detailed design.....	42
5.6.4.	Moving actuator	44
Conclusions.....		45
References.....		46
Appendices		47
	Appendix A: results measurements prototypes.....	47
	Appendix B: derivation transfer function	48
	Appendix C: Mass analysis of the concepts and final design	49
	Appendix D: Other design aspects concepts	50

Introduction

Demcon is developing custom designed actuators for a medical company. The actuators are used in a vest worn by patients who suffer from cystic fibrosis. The actuators create oscillating forces on the patient's thorax that helps to loosen the mucus in the lungs. This can be coughed up at a later stage.



Figure 1: a) Prototype of the therapeutic vest, b) Transversal cross section of the prototype ^[1]

Oscillating forces are obtained by accelerating a moving balance mass towards and away from the patient's thorax. The force created by this principle is called the Lorentz force. The oscillating forces have specific waveforms (force profiles) that are dependent on the preferences of the patients regarding frequency content and peak force magnitude.

Demcon has already realized a first prototype of the actuator which performs well in a prototype therapeutic vest. Three observations are made. First, for future series production it is essential to understand how variations in actuator parameters influence the waveforms and the magnitude of the therapy forces. Second, the force profile that is used in the prototype is based on an educated guess which might not be the most efficient force profile. Third, the therapeutic vest including the current design of the actuator is found heavy by the test users.

As first part of the assignment, a sensitivity analysis on the influence of variations in the actuator parameters on the waveforms is performed. These actuator parameters are: mass of the moveable body, stiffness of the springs that are used to connect the moveable body to the static part of the actuator, coil resistance, coil inductance, and the (position dependent) motor constant. This sensitivity analysis is done using simulations in Matlab/Simulink, and analytically using the Taylor series expansion. This Matlab/Simulink model needs to be optimised and the tolerances of the parameters are determined. After that, it is investigated if the force profile can be further optimised. As last part of the assignment, a redesign of the actuator is made in order to lower weight. This redesign is based on an adjusted list of requirements.

Some background information about the current design of the actuator is given in *Chapter 1*. After that a sensitivity analysis is performed in *Chapter 2*, the waveform optimisation is described in *Chapter 3*, and in *Chapter 4* an assumption is validated. Finally, *Chapter 5* describes the process and result from the redesign.

Chapter 1: Analysis of the actuator

The therapeutic vest consists of eight voice coil actuators, four at the back and four at the chest of the patient. The main function of those actuators is to deliver a therapy force on the patient's thorax according to a predefined force profile. The therapy force is delivered between a moving balance mass and the patient's thorax. This moving mass is the moving magnet assembly of the voice coil actuator.

1.1. Mechanical design of the actuator

After some research and calculations, a mechanical design for the actuator is made as shown in *Figure 2*. This consists of a moving back iron, a ring shaped permanent magnet which is magnetised in the radial direction, and two membrane springs that connect the moving body to the static part on which a coil is placed. A voice coil actuator can deliver a force according to the Lorentz force principle. Due to a current flow in the coil, a force is created if the coil interacts with the magnetic field due to the permanent magnet. The back iron is necessary to guide the magnetic field. This magnetic field will produce a force that will move the moving body with respect to the static part with the coil.

The actuator is designed in a way to fulfil the customer requirements and of course must be safe. The coil is intended to never impact the back iron or magnet. This is realised by using rubber end stops and using a linear guidance by two membrane springs. These springs have actually two functions, act as a linear guiding of the moving body, and give the system a specific resonance frequency to keep the power consumption low.

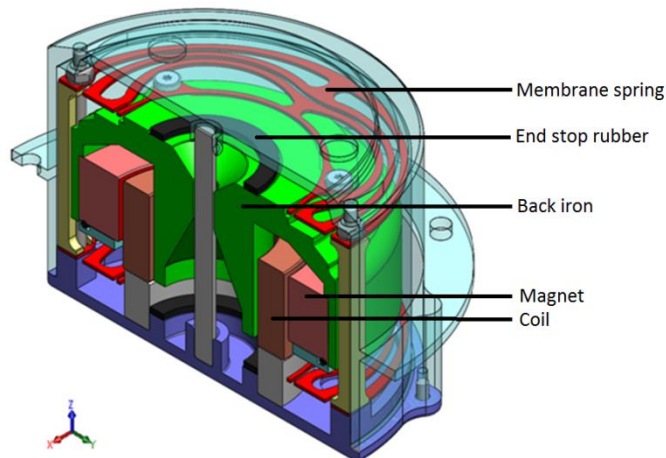


Figure 2: Mechanical design of the voice coil actuator ^[1]

1.2. Actuator requirements

The design of the voice coil actuator is based on a list of requirements from the customer. It should be small sized, low weight, low dissipated power, high impulse, low cost and of course be safe. The main requirements are listed below:

- 8 actuators (4 at the chest and 4 at the back) are required.
- Therapy frequency (=number of therapy force pulses per second) can vary between 5 and 20 Hz.

- Peak therapy force must be adjustable from 3 to 30 N in steps of 3 N and must be achievable for all therapy frequencies.
- Supply voltage to the actuators is 24 V at maximum.
- Actuators are intended to be used horizontally but tilt angles up to $\pm 30^\circ$ with respect to the horizontal line are allowed.

The requirements that the actuators should be low weight and have a small dissipated power are trade-offs. If the weight is really low, the accelerations and consequently the displacement of the moving body needs to be high to be able to produce the desired force. This follows from Newton's second law ($F = ma$) and the relation between acceleration and displacement: $x = \frac{1}{2}at^2$. A large displacement will make the vest very big and thick, which is also undesired. A good compromise between those variables is made.

1.3. Therapy force waveform generation

The therapy force is applied in a waveform that will give the desired therapy force at the desired therapy frequency, and is efficient. The force profile used for the actuator is shown in *Figure 3*. When the therapy frequency is very low, there is some waiting time (t_w) between the pulses. During that waiting time, the membrane springs are stretched what will cause a lot of dissipated power. To avoid this, some position correction is added to the signal. This will put the moving body back to its equilibrium position during the waiting time to decrease the dissipation as shown in *Figure 3b*.

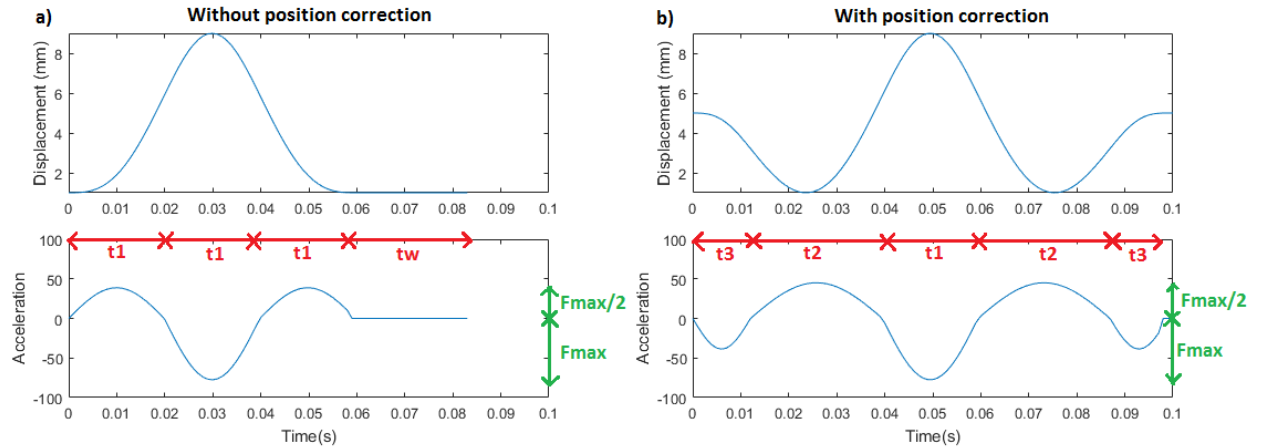


Figure 3: Waveform of the desired therapy force a) for high frequencies, b) for low frequencies

1.4. Engineering formulas for actuator optimisation

For the design of the actuator, some basic formulas are required. The major design criterion is to optimise the actuator to achieve a high efficiency over weight ratio. The efficiency is expressed as the second power of the force in $[N^2]$ per Watt dissipated electrical power. Hereby can the actuator force F_{act} be calculated using: $F_{act} = n_{windings} B I D_{coil}$ and the dissipated power P using:

$P = I^2 R = \frac{F_{act}^2}{k_m^2} R$ where $n_{windings}$ is the number of active coil windings, B is the average magnetic flux density at the position of the coil, I is the electrical current going through the coil, D_{coil} is the average coil diameter, R is the coil resistance, and k_m is the motor constant. The coil resistance R

can be calculated using $R = \frac{4\rho n_{windings} D_{coil}}{d^2}$ and the motor constant k_m using: $k_m = \frac{F_{act}}{I} = n_{windings} B D_{coil}$ where ρ is the electrical resistivity of the wire material (copper) in [Ωm], and d is the wire diameter. Manipulating those equations will give a relation between the copper volume in the coil and the actuator force and dissipated power: $V = \pi^2 \frac{F^2 \rho}{B^2 P}$.

1.5. The model

Next to those engineering formulas, a simple model describes how the actuator is able to deliver the therapy force on the patient's thorax. The desired therapy force needs to be translated to an electrical signal (a voltage and current) which controls the actuator. To be able to do this, a dynamic model of the actuator is considered. This is related to the current by the motor constant ($F_{act} = k_m I$). This current is needed to find the voltage to control the actuator.

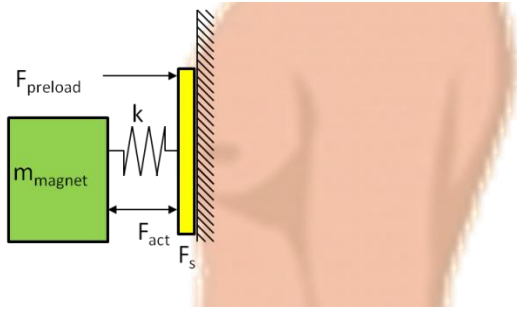


Figure 4: Simple model of interaction between patient's thorax and actuator ^[1]

The patient's thorax can be considered as a rigid body on which both the actuator force and the spring force that is executed by the membrane spring, are acting. These two forces are also acting on the moving assy as shown in Figure 4. This gives:

$$-F_{therapy} = -F_{act} - k \Delta x = m \Delta \ddot{x} \quad (1)$$

With F_{act} the actuator force, k is the spring constant and Δx is the displacement.

Another point of interest is the relationship between the driving current and voltage to realize the desired therapy force. The needed voltage to realise the therapy force consists of the voltage to overcome the resistance of the wire, the voltage to overcome the inductance of the wire, and the voltage to overcome the back electromotive force (back-EMF). We get the following relation^[1]:

$$U = U_R + U_L + U_{EMF} \quad (2)$$

Using the following expressions for the components of the voltage, this equation can be rewritten.

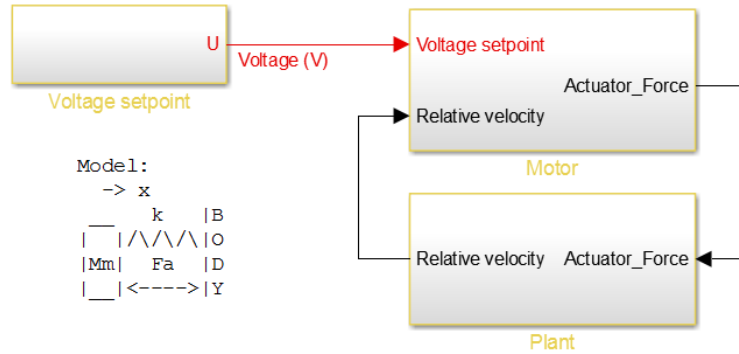
- The voltage caused by back-EMF, U_{EMF} : $U_{EMF} = k_m \dot{x}$
- The voltage caused by self-inductance, U_L : $U_L = L \frac{di}{dt}$
- The voltage caused by resistance of the coil, U_R : $U_R = IR$

A relation between the voltage and current appears by substitution these expressions in Equation (2):

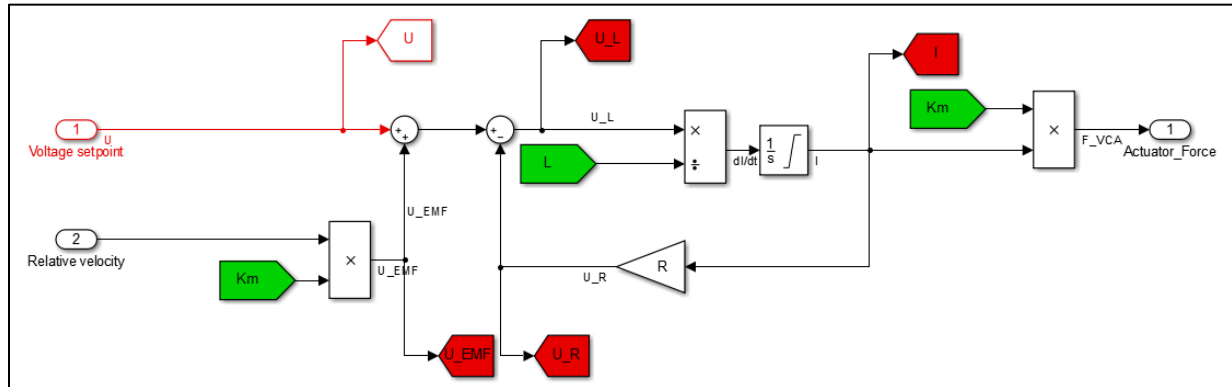
$$U = IR + L \frac{dI}{dt} + k_m \Delta \dot{x} \quad (3)$$

1.6. Matlab/Simulink model

Based on the data about the designed voice coil actuator, the requirements, the engineering formulas, the model, and the force profile, a Matlab/Simulink model is made. This model is schematically shown in *Figure 5* and shortly explained here.



Motor:



Plant:

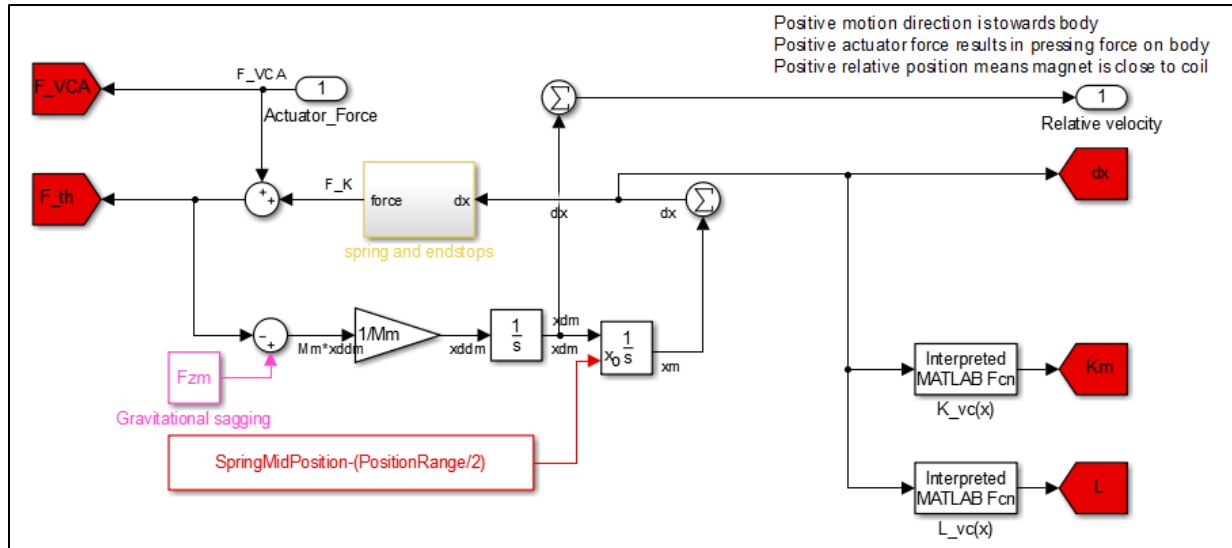


Figure 5: schematic representation the het Matlab/Simulink model of the voice coil actuator

This Matlab/Simulink model consists of three main blocks: voltage setpoint, motor, and plant. The first block, voltage setpoint, calculates the required voltage at every time step to create the desired therapy force profile. A sample frequency of 1 kHz is used, so one time step has a duration of 1/1000 second. The desired therapy force is set in the block voltage setpoint, from which the desired acceleration can be calculated (using $F_{therapy} = -ma$). Integrating the acceleration gives the velocity, integrating again gives the displacement. The actuator force can be determined using *Equation (1)* which is used to calculate the current ($I = F_{act}/k_m$). Then, the voltage setpoint can be calculated using *Equation (3)*. This is calculated for every time step and is send to the next block: motor.

The motor and plant combined represent the simulation which should give the same therapy force as set in the voltage setpoint. In the second block, motor, the calculations are executed in reverse direction. The current, and then the actuator force, is calculated from the voltages whereby the velocity comes from the plant. The simulated actuator force is output from the second block and goes to the third block, the plant.

The plant simulates the simple dynamical model as described above. This gives the velocity as output, which goes to the motor again.

The simulated therapy force should have the same values as the set therapy force. Unfortunately, this is not the case for all combinations of the desired therapy forces and therapy frequency.

Chapter 2: Sensitivity analysis

For the first part of the research, some questions about sensitivity are answered, and some improvements and optimisation opportunities in the model are investigated. The main aspects of the design of the actuator that are investigated are:

1. Discretisation problem: improvements on the model to make the simulated therapy force equal to the set therapy force.
2. Sensitivity analysis: the influence of some actuator parameters on the applied therapy force. Using this sensitivity analysis the worst case situation can be determined, and tolerances for the actuator parameters are set.
3. Analytical solution: comparing the simulation to the analytical results from a Taylor expansion.

2.1. Discretisation problem

The simulated therapy force applied by the actuator is in most cases higher than the therapy force set point. These deviations appear to be around the 3-4% for all settings (all combinations of 5 to 20 Hz therapy frequency and 3 to 30 N therapy force). These deviations are probably caused by the way the set point signal is generated: by discretisation of the continuous signal. This will cause deviations in the set point signal on which the simulation is based. This will also cause deviations in the simulated signal as shown in *Figure 6*.

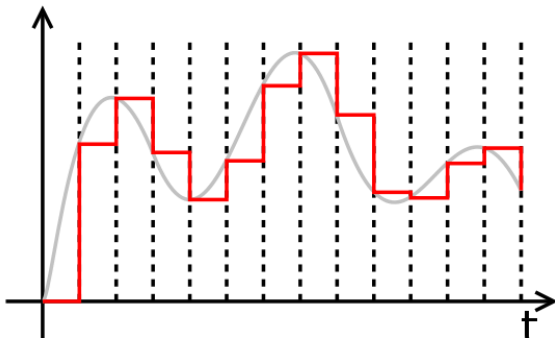


Figure 6: Discretisation(red) of a continuous signal (grey) gives deviations in the set point signal

In the final product, only a deviation of 5% in the therapy force is allowed. It is not desired to have a deviation of 4% due to a non-optimised set point signal, since there will always be other deviations caused by variations in actuator parameters, influence of the body, manufacturing errors etc. So this deviation in the model should be as small as possible.

Before executing a sensitivity analysis, this discretisation problem should be solved. To analyse the deviations caused by discretisation, the simulated therapy force is calculated for all 160 possible settings and the deviations from the set point is calculated for every combination of settings. This gives a 3D plot of the deviations as function of the therapy frequency and the therapy force. This plot (see *Figure 7*) gives insight in the relation between the set therapy frequency, set therapy force and the deviation in therapy force. This discretisation problem can be solved using three methods:

1. Use a higher sample frequency
2. Correct for the deviation with a correction factor based on a function fit of the 3D plot.
3. Correct for the deviation with a correction factor based on the simulated therapy force for every possible setting. This correction factor is stored in a look-up table with the perfect correction factor for every possible setting.

The results of those three solutions are investigated and compared to each other to select the most suitable solution.

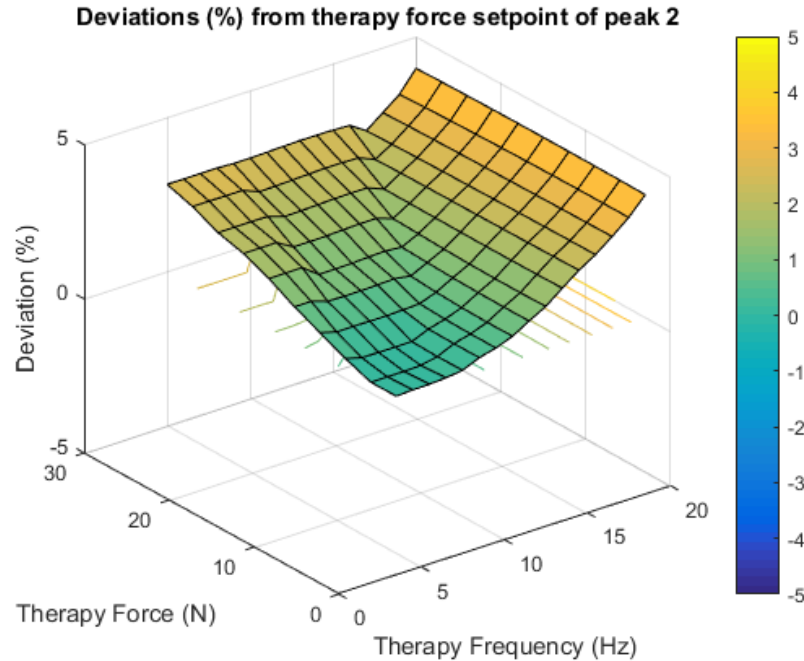


Figure 7: 3D plot of the deviations from the therapy force set point

2.1.1. Solution 1: Higher sample frequency

A sample frequency of 1000 Hz is used to create the set point therapy force. This will create a discrete signal which approaches a continuous signal. The higher the sample frequency, the better this continuous signal is approached and the better the simulated therapy force in the 'plant model' will approach the desired therapy force signal. To investigate the influence of the sample frequency on the deviations from the therapy force set point, the deviations for all possible combinations of settings are calculated for a sample frequency of 1000 Hz, 2000 Hz and 5000 Hz. The results are shown in *Table 1*. From these results it can be seen that increasing the sample frequency will indeed decrease the deviations from the therapy force set point.

Table 1: Deviations of therapy force for different sample frequencies

Sample frequency (Hz)	Deviation range (%)
1000	0.07963% to 4.013212%
2000	-0.01642% to 1.977735%
5000	-0.0119% to 0.788092%

2.1.2. Solution 2: Correction factor based on function fit

Using Matlab Curve Fitting Tool, an equation that fits the plot shown in *Figure 7* is determined. This equation is a polynomial equation of order 3 of the form:

$$deviation(x, y) = p_{00} + p_{10}x + p_{01}y + p_{20}x^2 + p_{11}xy + p_{02}y^2 + p_{30}x^3 + p_{21}x^2y + p_{12}xy^2 + p_{03}y^3$$

With x the Therapy Force (N), y is the Therapy Frequency (Hz), and p_{ij} are constants:

p00=-0.2547;	p01=0.04184;	p11=-0.001511;	p30=0.00004729;	p12=-0.0002181;
p10=0.02498;	p20=0.005192;	p02=-0.005853;	p21=0.00008501;	p03=0.0008022;

This polynomial equation gives approximately the deviation of the simulated value from the set point value (R-square = 0.9716). To correct for this real deviation, this calculated deviation is subtracted from the therapy force in the Simulink model. This is done by adding a gain in the 'Matlab/Simulink model, plant' (*Figure 5, plant*). This gain is added just before the red 'goto'-flag of 'F_th'. The gain is equal to: $gain = \frac{100}{100+CorrFac}$ where $CorrFac$ is the deviation in percentage.

With this correction factor the deviations appear to lie between -0.42988% and 0.322862% for a sample frequency of 1000 Hz. There is still a deviation present because not the real deviation is used as correction factor but the results from the Curve Fitting polynomial, which does not fit everywhere equally well.

The same procedure is used to find an equation for the correction factor ($CorrFac$) by using a sample frequency of 2000 Hz. This gives deviations between -0.2241% and 0.1416% from the set therapy force. The deviations lie between -0.0904% and 0.055593% for a sample frequency of 5000 Hz. So applying a correction factor based on a function fit will decrease the deviations. This can be decreased even further by increasing the sample frequency.

2.1.3. Solution 3: Correction factor based on a look-up table

The deviation is calculated for every possible combination of settings. The results can be saved in a table and be used to correct for this error. This gives a 10x16 table in which the correction factors can be found for every setting. This correction factor is applied in the same way as the correction factor with the function fit in 'Solution 2'. By applying this correction factor, the deviations are always equal to zero. This is obvious since the exact deviation is subtracted.

2.1.4. Solution selection

As shown above, all three solutions cause a decrease in deviation from the therapy force set point. To choose the best suitable solution, the results are compared to each other. A requirement from the customer is a maximum sample frequency of 1000 Hz. Increasing this is only an option, if there are no other solutions to the problem, which there are. To make a decision between the other two correction methods, the efficiency and applicability is taken into account. There is already a look-up table present in the model, so it is easy to add an extra table to it with the correction factors. By doing this, the therapy force is always exactly equal to the set point. By using the function fit, there will still be some deviations. So 'solution 3: correction factor based on a look-up table' is chosen to compensate for the discretisation.

This is introduced in Matlab using some extra code where *dev* is the 10x16 table with the deviations:

```
CorrFac_table=load('deviations_peak2_SampleFreq1000','dev');
row=TherapyForce/3;
column=TherapyFreq-4;
CorrFac=CorrFac_table.dev(row,column);
```

This correction factor is implemented in the 'Matlab/Simulink model, plant' by using a gain:

$gain = \frac{100}{100+CorrFac}$ where *CorrFac* is the deviation in percentage, in front of the output *F_{th}*. This correction factor is applied to perform the sensitivity analysis to ensure that the measured deviation is only coming from variation in the parameters and not from the model anymore.

2.2. Sensitivity analysis

There are five important actuator parameters that can have deviations from the expected value. The five actuator parameters that are tested are:

1. The mass of the moving body *m*
2. The spring constant *K*
3. The resistance of the coil *R*
4. The motor constant *K_m*, this parameter is position dependent
5. The coil inductance *L_m*, this parameter is position dependent

The influence of every parameter is tested individually. It is assumed that all five parameters are completely independent of each other. The Matlab/Simulink model is adapted to make it easy to add some error on the values of the parameters. This is done by introducing an error value for all of them. Every parameter is tested with a deviation of +5% and -5%. So the original value is multiplied by (1.00+0.05) or (1.00-0.05). This is done for a set therapy force of 10N, 20N and 30N, with a therapy frequency of 5Hz, 12Hz and 20Hz. The results are summarized in *Table 2*. It is clear that the variations in mass, the coil resistance and the motor constant cause the biggest deviations in the therapy force. These tolerances should be made as small as possible to reduce the deviations in the therapy force.

Table 2: a) Percentage deviation in therapy force due to -5% variations in the five parameters (yellow: deviation is more than ±1%)

F _{th} f _{th}	10 N			20 N			30 N		
	5 Hz	12 Hz	20 Hz	5 Hz	12 Hz	20 Hz	5 Hz	12 Hz	20 Hz
m	-4.5930	-4.3810	-2.6140	-3.7140	-3.7435	-2.4765	-3.5690	-2.6293	-2.4707
K	0.2400	0.2910	-0.4250	0.2585	0.1205	-0.1660	-0.2527	0.4093	-0.0567
R	0.6950	1.1350	2.9400	1.6770	1.8320	3.1080	1.7263	3.0497	3.0870
K _m	4.0730	3.2730	-0.1450	2.2320	1.6660	0.1310	0.1163	-0.1843	0.0697
L _m	-0.1720	-0.5840	-0.4540	-0.2280	-0.5465	-0.2755	-0.6490	-0.1870	-0.2167

b) Percentage deviation in therapy force due to +5% variations in the five parameters (yellow: deviation is more than $\pm 1\%$)

F_th f_th	10 N			20 N			30 N		
	5 Hz	12 Hz	20 Hz	5 Hz	12 Hz	20 Hz	5 Hz	12 Hz	20 Hz
m	4.5970	4.1660	2.3960	3.8105	3.6105	2.6485	2.5633	3.0193	2.7020
K	-0.1980	-0.4700	0.3410	-0.0815	-0.2455	0.4810	-0.5837	0.2333	0.4440
R	-0.5930	-1.2280	-2.8390	-1.4665	-1.8010	-2.6195	-2.5107	-2.2803	-2.5473
Km	-3.9870	-3.3640	-0.3050	-1.9545	-1.8965	-0.2170	-1.2877	0.1130	-0.1287
Lm	0.3020	0.3970	0.3290	0.3495	0.4495	0.5525	-0.2417	0.7440	0.5643

From the results in *Table 2*, the worst case for every parameter is determined. By applying the worst case for every parameter, the worst case for the whole model can be determined (it is assumed that all the parameters are independent of each other). These results are shown in *Table 3* where the percentages are the deviations of the simulated therapy force from the set therapy force.

Table 3: Percentage deviation in therapy force in the worst cases

	10 N	20 N	30 N
5 Hz	10.0694%	8.2854%	5.8646%
12 Hz	9.8557%	7.8620%	6.6839%
20 Hz	6.2159%	6.4597%	6.3379%

The maximum allowable deviation in the therapy force is 5%, so the tolerances of the five parameters are investigated to see what the real deviations for every separate parameter are.

The standard deviation for every parameter is determined using the test results of 20 prototypes of the actuator, see *Appendix A*. The mean value μ and the standard deviation σ are determined for the resistance R , and the eigenfrequency ω_r . The deviation in the parameters is set to 3σ which covers 99.73% of the cases and can be calculated by: $dev = 3\sigma/\mu$. The variation in the spring constant can be calculated using the eigenfrequency: $K = m(2\pi\omega_r)^2$ where m is the mass of the moving body.

The results are shown in *Table 4*. Here are the motor constant Km and the inductance Lm a function of the displacement x , so these do not have a mean value and a standard deviation, but they got a deviation based on the curves as shown in *Appendix A*.

Table 4: Deviations in the parameters based on research on prototypes

Parameter	Mean value μ	Standard deviation σ	Deviation worst case
m	0.387 kg	-	1%
ω_r	12.440 s ⁻¹	0.1659 s ⁻¹	-
K	2364.3 N/m	64.0726 N/m	8.05%
R	3.8655 Ω	0.0332 Ω	2.57%
Km	-	-	5%
Lm	-	-	1%

The deviations as shown in *Table 4* are used to determine the worst case deviation in the therapy force again. The results are shown in *Table 5* which shows that mainly the combination of a low therapy frequency and a low therapy force gives too high deviations.

Table 5: Percentage deviation in therapy force in the worst cases based on prototype results

	3 N	12 N	21 N	30 N
5 Hz	7.7205%	5.3355%	3.8673%	2.5909%
12 Hz	5.5932%	5.4952%	3.5212%	2.3394%
20 Hz	2.7280%	2.7808%	2.7559%	2.5430%

After some trial and error by adjusting the tolerances, it can be concluded that it is not possible to decrease these tolerances and to get the deviation of the therapy force lower than 5% for all combinations of therapy frequency and therapy force. This gives the final and best tolerances as shown in *Table 4*.

2.3. Analytical solution

The influence of the five parameters can not only be tested in the simulation, but also using a Taylor series expansion. First the transfer function is derived (see *Appendix B* for the full derivation):

$$G(s) = \frac{F_{th}(s)}{U(s)} = \frac{k_m m s^2}{(R + L_m s)(m s^2 + k) + k_m^2 s} \quad (4)$$

A Taylor series expansion is performed with respect to the five parameters m, k, R, k_m and L_m around their nominal values ($m_0, k_0, R_0, k_{m0}, L_{m0}$). A Bode diagram is made for each parameter which will give insight in the sensitivity of the therapy force on those parameters. This should give a result similar to the sensitivity analysis as described before.

The total derived Taylor series expansion is:

$$\begin{aligned}
G(s) &= G_0(s) + \frac{\partial G(s)}{\partial m} \delta m + \frac{\partial G(s)}{\partial k} \delta k + \frac{\partial G(s)}{\partial R} \delta R + \frac{\partial G(s)}{\partial k_m} \delta k_m + \frac{\partial G(s)}{\partial L_m} \delta L_m \\
G(s) &= \frac{k_{m0} m_0 s^2}{(R_0 + L_{m0} s)(m_0 s^2 + k_0) + k_{m0}^2 s} \\
&+ \frac{((R_0 + L_{m0} s)(m_0 s + k_0) + k_{m0}^2 s) k_{m0} s^2 - k_{m0} m_0 s^2 (R_0 + L_{m0} s) s^2}{((R_0 + L_{m0} s)(m_0 s + k_0) + k_{m0}^2 s)^2} (m - m_0) \\
&+ \frac{-k_{m0} m_0 s^2 (R_0 + L_{m0} s)}{((R_0 + L_{m0} s)(m_0 s + k_0) + k_{m0}^2 s)^2} (k - k_0) \\
&+ \frac{-k_{m0} m_0 s^2 (m_0 s^2 + k_0)}{((R_0 + L_{m0} s)(m_0 s + k_0) + k_{m0}^2 s)^2} (R - R_0) \\
&+ \frac{((R_0 + L_{m0} s)(m_0 s + k_0) + k_{m0}^2 s) m_0 s^2 - 2 k_{m0}^2 m_0 s^3}{((R_0 + L_{m0} s)(m_0 s + k_0) + k_{m0}^2 s)^2} (k_m - k_{m0}) \\
&+ \frac{-k_{m0} m_0 s^3 (m_0 s^2 + k_0)}{((R_0 + L_{m0} s)(m_0 s + k_0) + k_{m0}^2 s)^2} (L_m - L_{m0}) \quad (5)
\end{aligned}$$

For every transfer function belonging to one of the parameters, a Bode diagram is made and scaled to the nominal value of this parameter. The magnitude plot is shown in *Figure 8*. The deviation in therapy force per voltage due to a variation of 5% in every parameter is shown. These deviations are at a maximum for a frequency around 7-8 Hz.

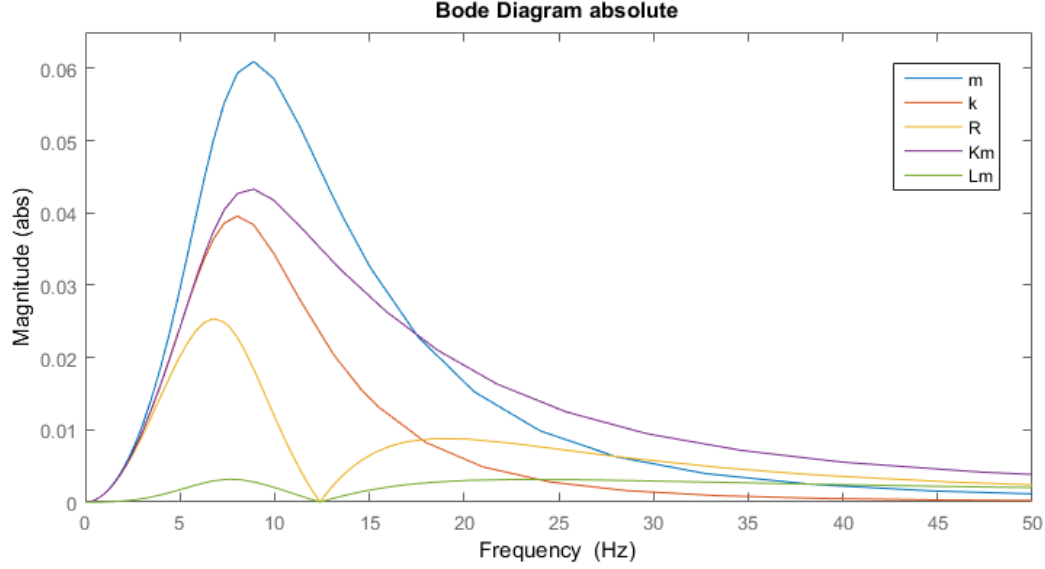


Figure 8: Magnitude plot of the Taylor series expansions; $|\partial G_0(s)/\partial m|/m_0$ (blue), $|\partial G_0(s)/\partial k|/k_0$ (red), $|\partial G_0(s)/\partial R|/R_0$ (yellow), $|\partial G_0(s)/\partial k_m|/k_{m0}$ (purple) and $|\partial G_0(s)/\partial L_m|/L_{m0}$ (green)

From this analytical analysis, it can be concluded that the influence of the inductance of the coil is very small and the influence of the mass is the biggest. This is similar to the result from the sensitivity analysis. The other parameters lie in between but not in the same order as followed from the sensitivity analysis.

Chapter 3: Waveform optimisation

A waveform is introduced in *Chapter 1*. This waveform gives good results, but it has not been investigated what other waveforms do and what the best way is to add a position correction to the waveform. These two aspects of the waveform are investigated.

3.1. Testing new waveforms

For the cases with higher therapy frequencies, the position correction is not applied. Three other waveforms are investigated for these situations and the results are compared to the original waveform. These other waveforms are shown in *Figure 9*. For the therapies at low frequencies, the original position correction is adjusted to get the best result by adjusting the amplitudes of the peaks. Also, another simple way of position correction is investigated and compared to the original optimised position correction. This simple position correction is created by adding a sinus in front of the acceleration signal of the acceleration. This will cause the magnet to move back to its equilibrium position at 5 mm. This is shown in *Figure 10* together with the original position correction.

The results of the waveform are compared to each other on a few factors. First, the displacement Δx must be within acceptable ranges. Second, the impulse (i.e. the integral of the positive part of the therapy force over time) must be as big as possible. This is reached when the therapy time t_{therapy} is as long as possible. This therapy time is the time duration of the positive part of the therapy force. Third, the power dissipation must be kept small. Based on this, the most efficient waveform is selected.

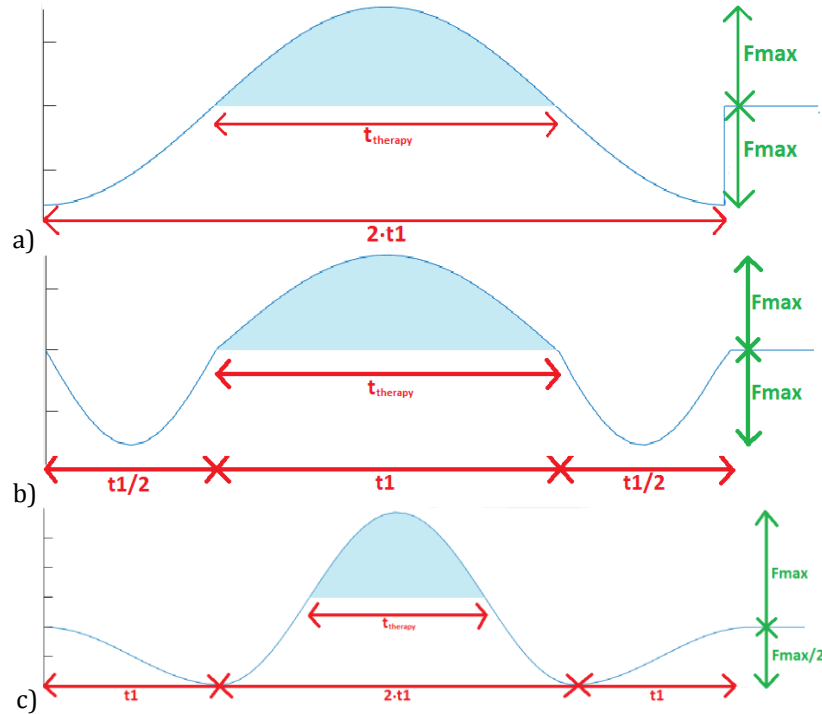


Figure 9: a) Alternative waveform 1 (cosine), b) alternative waveform 2 (three parts of a sine), c) alternative waveform 3 (three parts of a cosine). Impulse is light blue area.

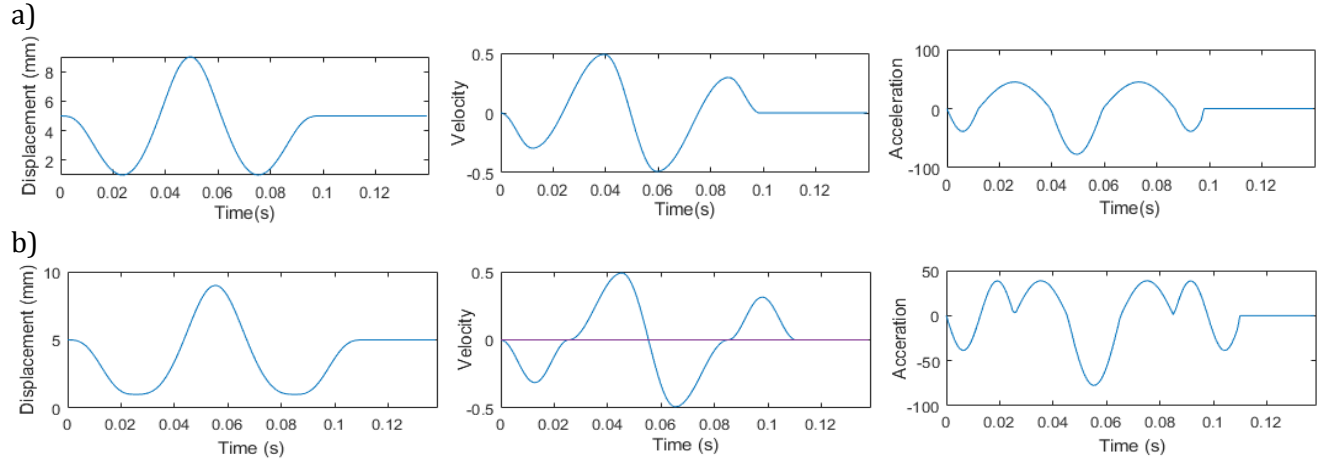


Figure 10: Position correction for the original waveform a) original position correction b) simple position correction

The four waveforms (the original and the three new waveforms) are tested at a therapy frequency of 5 Hz and 20 Hz. For the 20 Hz simulations there is no position correction applied and for the 5 Hz simulations the simple position correction is applied. The results are shown in *Table 6*. All waveforms create displacement within the boundaries. The original waveform and waveform 3 show similar and the lowest dissipated power for both therapy frequencies.

Table 6: waveform analysis

		Original	Waveform 1	Waveform 2	Waveform 3
5 Hz (simple PosCorr)	P_{diss} (W)	1.0283 W	1.6205 W	1.7601 W	1.1562 W
	$t_{therapy}$ (s)	0.0199 s	0.0226 s	0.0239 s	0.0171 s
	Δx (mm)	1 – 9 mm	1 – 9 mm	1 – 9 mm	1 – 9 mm
20 Hz (Without PosCorr)	P_{diss} (W)	2.2553 W	4.2198 W	5.1077 W	2.4472 W
	$t_{therapy}$ (s)	0.0167 s	0.0226 s	0.0239 s	0.0167 s
	Δx (mm)	2 – 8 mm	1 – 9 mm	1 – 9 mm	3 – 7 mm

3.2. Optimising original waveform

The original waveform had a position correction with a sine with amplitude $amax/2$ but the displacement is not within the boundaries (the moving assy will touch the end stops). The amplitude and the period of this sine can be optimised to get the best allowable results. The durations of the three peaks, as defined in *Figure 3*, and the amplitudes of the three peaks are dependent of each other whereby the amplitude of the peak that causes the therapy force is set. The others can be determined using some boundary conditions:

- At time $t = t_3 + t_2$ (at the start of the therapy peak) the acceleration should be equal to zero for both cases, with and without position correction. So the velocity and the displacement of the moving body with position correction should be equal to respectively the velocity and the displacement without position correction.
- At the point where the velocity is equal to zero, the displacement should be equal to its minimum, which is set to 1 mm in the actuator.

The amplitude a_{max} of the therapy peak is set and $t_{therapy}$ is determined. Using this, a system of three equations with four variables and multiple solutions is obtained. Two of the other variables can be chosen to solve the system of equations, this is done by choosing one variable and iterating a second until the best result is obtained.

The best result for the original waveform is obtained for:

```
m = 1.72167; % amplitude factor during t2
n = 2.0; % amplitude factor during t3
a = -2.0/m-2.0*n/m/m;
b = 2.0*t1+2.0*t1*n/m;
c = -n/2.0*t1*t1-t1*t1+pi*xmax/amax;
t2 = -b/2.0/a-sqrt(b*b-4.0*a*c)/2.0/a;
t3 = n/m*t2-n/2.0*t1;
```

Here is the amplitude of the peak during t_3 equal to a_{max}/n and the amplitude of the peak during t_2 equal to a_{max}/m as shown in *Figure 11*. This result shows that the original waveform using the optimised position correction can be improved even more. The dissipated power is equal to 0.9709 W for a therapy frequency of 5 Hz and the moving assy moves within the boundaries now.

From this it can be concluded that the original waveform with the optimised version of the position correction gives the best results. The dissipation is the lowest, and $t_{therapy}$ is bigger than for waveform 3, so the impulse will be higher. The moving body will also stay within the boundaries and is able to move safely in the actuator without touching the end stops.

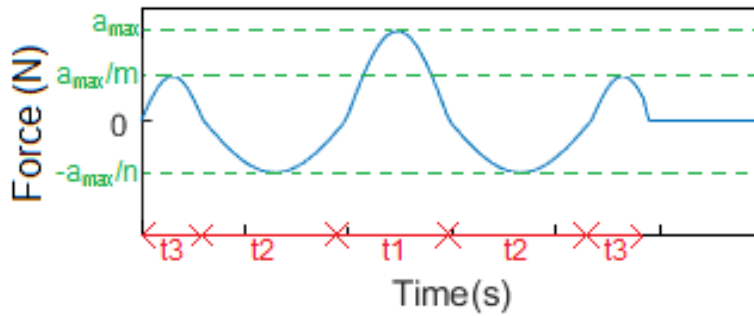


Figure 11: Force profile with a_{max} as measure for the magnitude of the force

Chapter 4: Verifying the assumed rigid thorax

In the model it is assumed that the thorax is a rigid body which is not the case in reality. A new model is made which also included the effects of the body. The tissue is modeled as a spring and a damper. The weight of the tissue and the stationary part of the actuator together is called m_c , and the moving part of the actuator is m_m . The dynamic model is shown in *Figure 12* and expressed in *Equation (6)*. The Matlab/Simulink model is adjusted to this dynamic model by modeling *Equation (6)* in the 'Plant' in Simulink as shown in *Figure 13*.

$$\begin{cases} k_{spring}(x_m - x_c) + F_{act} - k_{skin}x_c - c_{skin}\dot{x}_c = m_c\ddot{x}_c \\ -k_{spring}(x_m - x_c) - F_{act} = m_m\ddot{x}_m \end{cases} \quad (6)$$

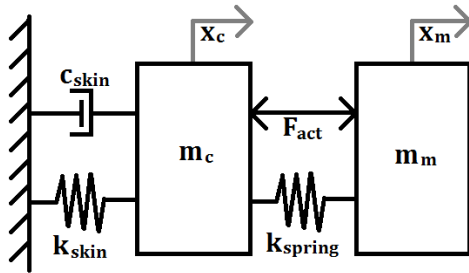


Figure 12: Dynamic model with compliant tissue

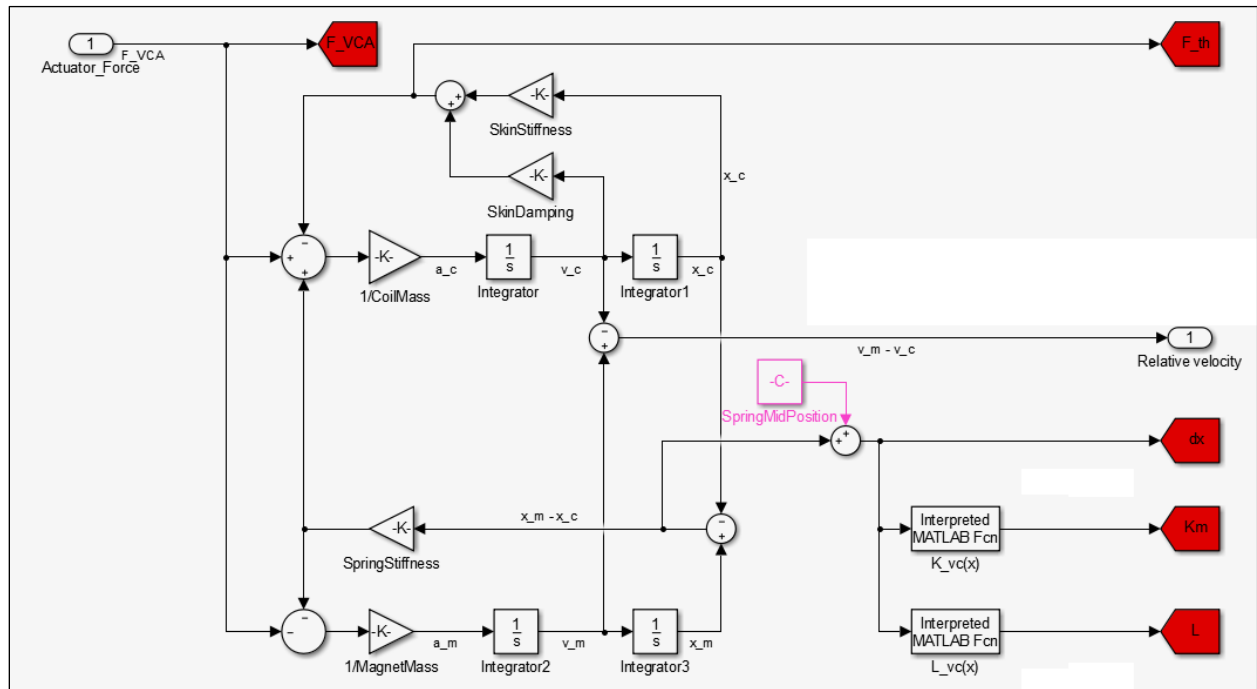


Figure 13: Adjusted 'Plant' in the Matlab/Simulink model

The tissue is modeled as a spring and a damper, this means that the elastic properties of human tissue need to be translated to a spring stiffness and a damping constant. It is complicated to determine an exact value for the stiffness and the damping since tissue is different from person to person and dependent on environmental conditions. The elastic modulus of skin depends on the

age, gender, body mass index, types and percentages of tissue in the tissue layer, hydration, thickness of the tissue layer, and location on the body.

An approximation for the mass of the tissue is made using the diameter of the actuator (7 centimeters), a thickness of 1 centimeter tissue and a density of tissue of 1050 kg/m^3 . This gave a mass of the tissue of 40 grams. The mass of the stationary part of the actuator is 150 grams according to the original Matlab/Simulink model. This gives a total mass of 190 grams for m_c .

It is known that tissue causes an overdamped system, so the damping ratio ζ (zeta) has to be bigger than one: $\zeta > 1$. According to Amar M.R.S. [2] the damping constant has a value of $c_{skin} = 1.824$ and the spring stiffness $k_{skin} = 18500 \text{ N/m}$. This gives a good order of magnitude to start the simulations. The influence of the damping ratio and the stiffness on the simulated therapy force is investigated by varying these parameters. The damping ratio is varied between 1 and 2. This showed a smaller range of deviations in the simulated therapy force from the set therapy force for higher damping ratios. This also caused a small increase in dissipated power. The stiffness of the tissue is varied between 750 N/m and 150000 N/m . This showed smaller deviations and higher dissipated power for stiffer material (higher stiffness).

All deviations of the simulated therapy force are negative, so the actual applied force is less than desired. For all tested damping ratios and stiffness higher than 10000 N/m , this deviation is always smaller than 5%, as shown in Figure 14. Also the dissipated power stays low as shown in Figure 14. If the thorax has a stiffness higher than 1000 N/m , the deviation will always be smaller than 20%.

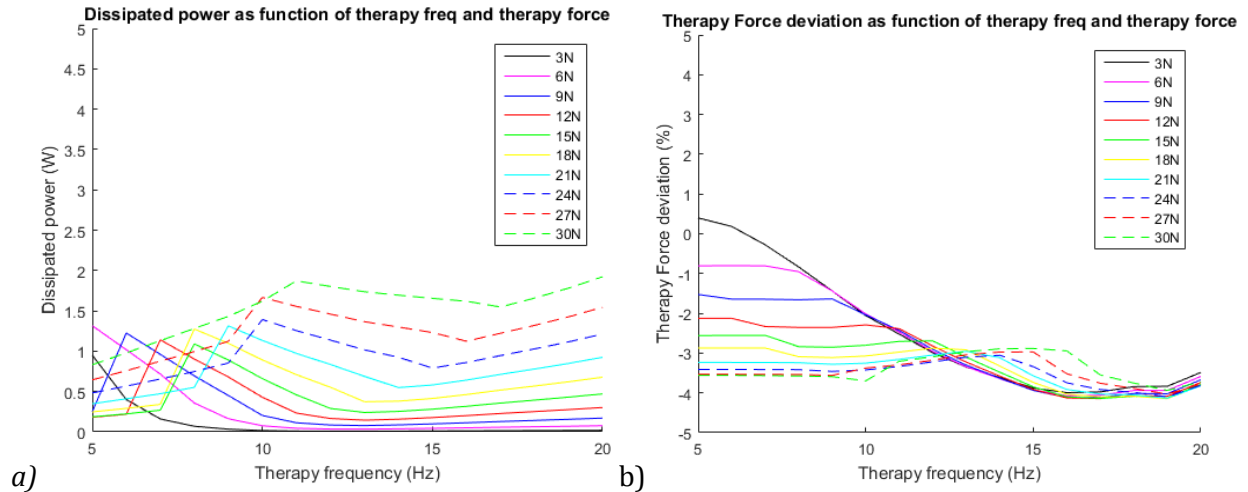


Figure 14: a) Dissipated power, b) deviation as function of the therapy force and therapy frequency for $\zeta = 1.5$, $k = 10000 \text{ N/m}$, $m_c = 0.190 \text{ kg}$

Chapter 5: Redesign of the actuator

The current design is based on the requirements given in *Chapter 1*. But the customer has new requirements after testing of the current design on patients. The design of the actuator is adjusted to these new requirements. The patients said that the vest with the actuators was very heavy, and that they were satisfied with a therapy force of 18N. Based on this, some new requirements are set:

- The maximum mass of the actuator is 350 grams (instead of 550 grams)
- The maximum dissipated power is increased to 3 W
- The therapy force range, therapy frequency range and the therapy time may be adjusted within acceptable range to reach the mass reduction.

A few steps are needed to accomplish a redesign of the actuator. These steps are:

1. Use the Matlab/Simulink model to determine acceptable reductions in motor parameters, therapy force, therapy frequency, and therapy time. These are chosen in such a way that the maximum dissipated power stays at 3W.
2. Use the program FEMM to simulate the actuator with the chosen parameters and adjust the dimensions of the back iron and magnets in such a way that it can deliver the desired force without exceeding the maximum dissipated power. This can be checked by simulating the actuator with the found dimensions and properties in the Matlab/Simulink model. These steps are repeated until the desired result is reached. After that, a design for the back iron, the magnets, and the coil are made.
3. This functional design is used as a starting point for the further design of the actuator. Concepts for a pretension spring, and linear guidance of the moving body are designed and presented in a morphological diagram.
4. Ranking the solutions and combining those, will give some concepts. These concepts are drawn in SolidWorks.
5. The concepts are ranked again and the concept with the best score is used for the final design.

These steps are described in this chapter.

5.1. Reduction of the motor parameters and therapy parameters

It is complicated to reduce the mass and keep dissipated power the same as for the current actuator design without adjusting motor parameters and desired therapy force, therapy frequency, and therapy time. The influence of the parameters is analysed in *Chapter 2* and can be used as a guideline to set a target for the mass reduction. This should give a realistic result for the actuator.

Since patients indicated that they were satisfied with a therapy force of 18N, the therapy force range can be reduced to 3N – 24N. This is beneficial because the highest dissipated power is present for high therapy forces. By eliminating the highest therapy forces, the maximum dissipated power stays within range. The allowable reduction in therapy time is set to 10% to keep the impulse high.

The dissipated power is also dependent on the therapy frequency. At higher therapy frequencies, the dissipation is higher. But this effect is less important than the influence of the therapy force. If necessary, the therapy frequency range might be reduced to 5Hz to 18Hz.

As starting point, the allowed mass is divided over the different parts of the actuator based on the ratio of mass in the current design:

- Mass back iron (including magnets): 250 gram
- Mass coil: 50 grams.
- Mass housing: 50 grams.

Based on these masses and the set reductions of therapy parameters, a reduction of the other motor parameters is estimated. These are simulated in the Matlab/Simulink model to investigate the influence on the dissipated power and the therapy force range. This is done for different combinations of reductions in the motor parameters and gave some limits that can be used as starting point for the design.

Using the set limits in therapy parameters, it can be concluded that the motor constant may be reduced to 75% of the original value, the coil resistance may be reduced to 75% of the original value, and the stiffness should be kept approximately unchanged. The stroke is set to 10mm and the coil inductance is neglected here since the influence is very small.

5.2. Functional design in FEMM

The results from the Matlab/Simulink simulation and the reductions in parameters are used as starting point. The size and shape of the back iron, the magnets and the coil are designed in the program FEMM. The dimensions and number of windings of the coil can be calculated using Equation (7).

$$R = \frac{4\rho n_{windings} D_{coil}}{d^2} \quad (7)$$

Using a simulation, the saturation of the back iron and the Lorentz Force (which is equal to the motor constant for $I = 1A$) can be determined. Using iteration, a relation between the motor constant and the position of the back iron is determined.

The shape of the back iron is optimised to reduce weight but still has some useful design features for later production. Two examples are: a small edge to place the magnets precisely against the back iron, and a protuberance for guidance of an axis in the middle of the actuator. The calculated motor constant is shown in *Figure 15* and has an average of 80% of the original value. The design is shown in *Figure 16*.

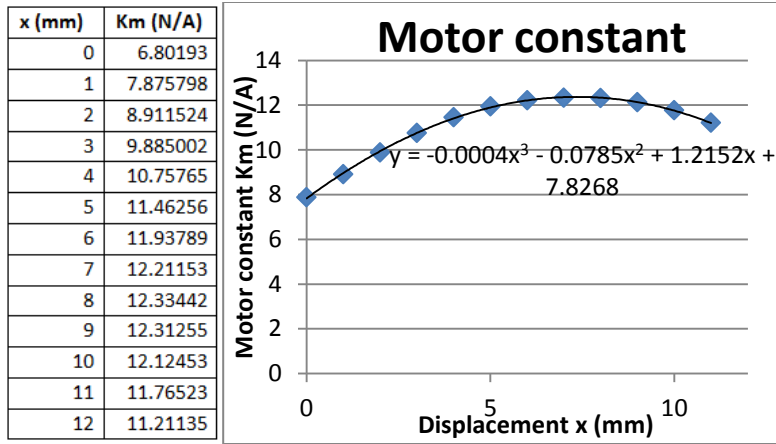


Figure 15: Calculation motor constant for the functional design in FEMM

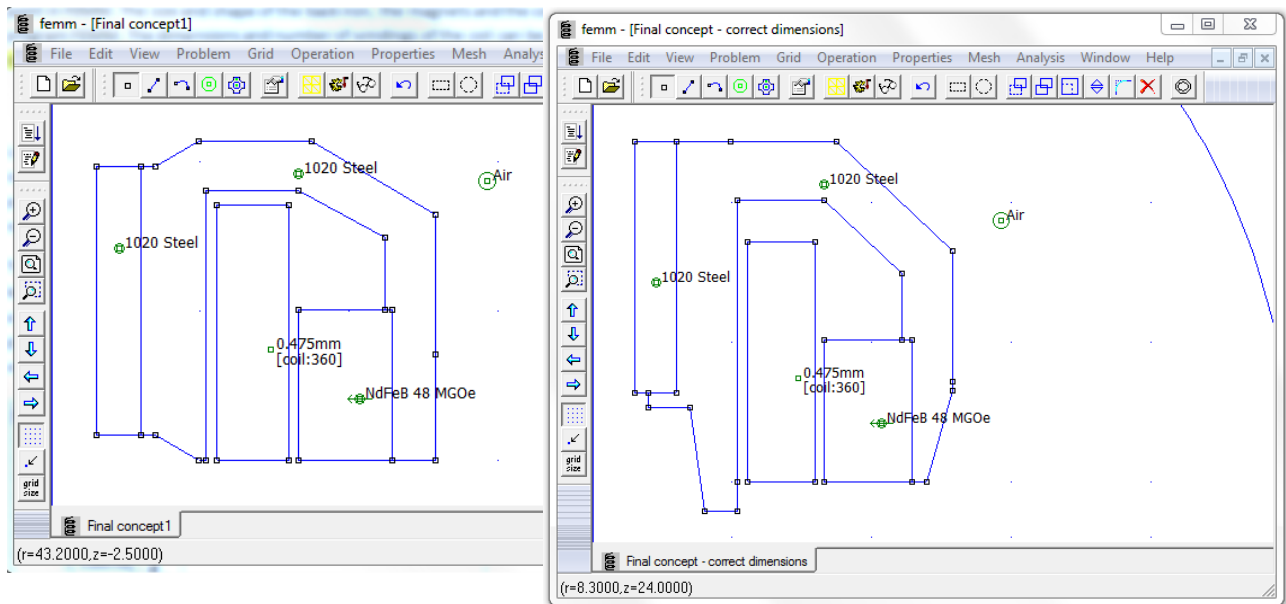


Figure 16: Design of the back iron, magnets and coil in FEMM (left: starting point, right: final design)

Putting the equation for the motor constant in the Matlab/Simulink model, together with the correct mass and resistance, will give the influence on the dissipated power and the therapy duration. The design fulfils the set requirements as shown in *Figure 17*.

The final design is based on the reduced values of the motor parameters and the therapy parameters. The motor constant and the coil resistance have values of 80% and 76% of the original values respectively, and the stroke is set to 10mm. The therapy force range is reduced to 3N – 27N, and the therapy time is 96% of the original time. The therapy frequency range is not reduced.

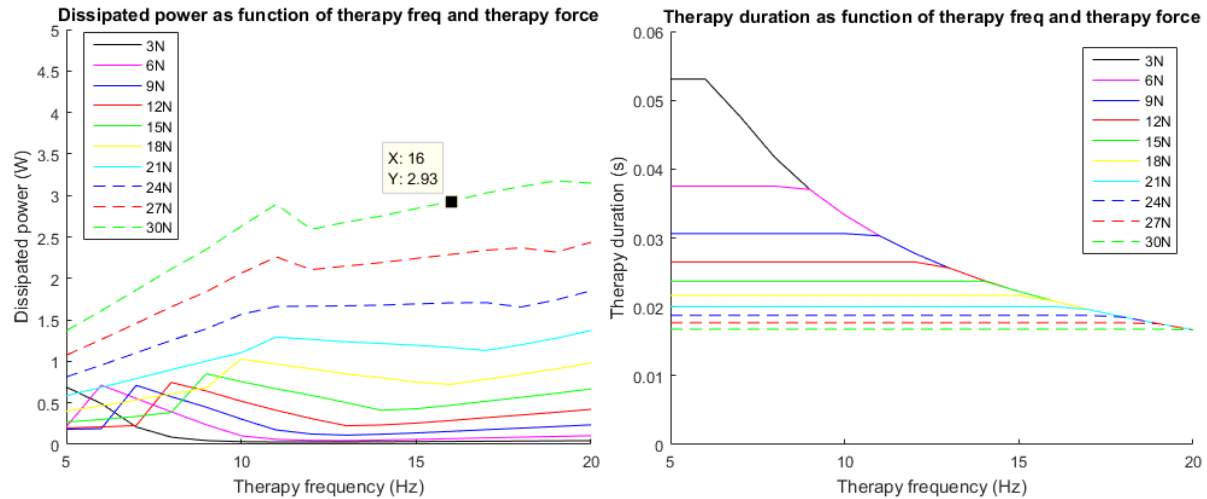


Figure 17: a) dissipated power and b) therapy duration as function if therapy frequency and therapy force with reductions of functional design

5.3. Morphological diagram

There are other aspects that need to be designed next to the functional design. Two important sub problems are:

- Pretension is needed in the actuator to control the position.
- Linear guidance of the moving body to avoid forces and lost power in undesired directions.

Solutions for those sub problems are shown in a morphological diagram (Table 7 and Figure 18) and explained below. After designing this, concepts are assembled and the best concept is selected. Then some other connections between parts in the actuator can be designed.

Table 7: Morphological diagram in words

Function:	Solution 1	Solution 2	Solution 3	Solution 4	Solution 5
Pretension	Two custom made compression-extension springs (one on top, one at the bottom)	Two compression springs (one on top, one at the bottom)	Parallel compression springs (multiple springs on top, multiple at the bottom)	Extension spring on top, compression spring at the bottom	Two leaf springs (one op top, one at the bottom)
Linear guidance	Sliding contact linear motion bearing	Rolling element linear motion bearing	Elastic bearing (leaf springs)	Hydrostatic/aerostatic linear motion bearing	Magnetic linear motion bearing

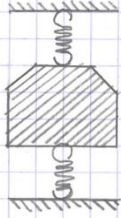
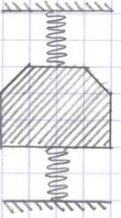
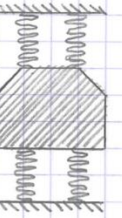
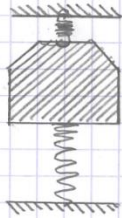
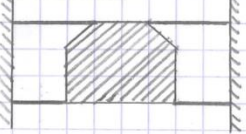
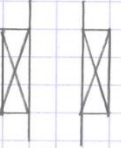
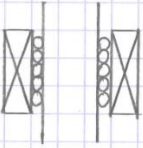
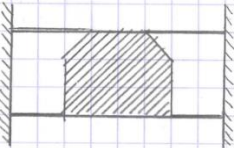
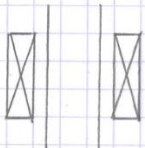
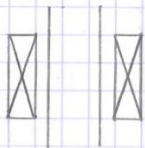
Function:	Solution 1	Solution 2	Solution 3	Solution 4	Solution 5
Pretension					
Linear guidance					

Figure 18: Morphological diagram

5.3.1. Pretension

There are five mean solutions to create pretension in the actuator using springs. The advantages and disadvantages of these solutions are explained here. Also, some basic calculations are performed to see if the solution is feasible.

Solution 1: custom compression-extension springs

The dimensions for the compression-extension spring are calculated using the spring calculator as shown in *Figure 19*. But the desired deflection for the springs is only half of the total stroke for these springs since the equilibrium position of the spring is also the equilibrium position of the moving body. If the stroke is divided in two, the spring force is also half the size. This will give dimensions of the spring as shown in *Table 8* where L_c is the length of the spring in compressed state, and L_0 the length of the spring in equilibrium position. This gives the dimensions for two springs in parallel, one on top of the back iron and one at the bottom. Another option is putting more springs in parallel. The dimensions of the springs for six in parallel are also shown in *Table 8*.

$d=0.32 \cdot 10^{-3};$	%diameter of the wire (m)
$D=3.2 \cdot 10^{-3};$	%mean diameter of the spring (m)
$n=14;$	%number of active coil windings (-)
$G=79.3 \cdot 10^9;$	%shear modulus
$F=2.54;$	%spring force (N)
$L_c=n \cdot d;$	%spring length compressed (m)
$f=64 \cdot n \cdot (D/2)^3 \cdot F / (d^4 \cdot G);$	%spring deflection (m)
$k=F/f$	%spring stiffness (N/m)
$L_0=L_c+f;$	%spring length free/equilibrium (m)
$\sigma=F \cdot 16 \cdot D/2 / (\pi \cdot d^3) / 10^6$	%average stress (N/m ²)

Figure 19: Dimension calculator for springs ^[3]

Table 8: Dimensions of compression-extension spring

	2 parallel (1 top, 1 bottom)	6 parallel (3 top, 3 bottom)
	Calculator	Calculator
d (mm)	0.77	0.40
D (mm)	8.0	5

n (-)	9	8
F_{max} (N)	3.8	1.27
L_c (mm)	6.93	3.2
f (mm)	5.03	5.00
k (N/m)	756	254
σ (MPa)	169.6	253
L_0 (mm)	11.96	8.2

Compression-extension springs need to be custom made since they are not found in a catalogue of suppliers. This is a disadvantage since it will increase the production costs for the springs. Furthermore, these springs need to be attached between the stationary and moving body. This can be done by clamping with a linear shaft support block or with a wire robe clamp as shown in *Figure 20*. This is integrated with the back iron and assembled on top and on the bottom of the stationary body.



Figure 20: Example of a) a linear shaft support block, b) wire robe clamp

Solution 2: Two compression springs

Compression springs are used instead of compression-extension springs. This will increase the deflection the spring should withstand to 10mm. An advantage is that compression springs are widely available in all kind of dimensions and stiffness.

Using some calculations and iteration, some dimensions for suitable springs are obtained using the spring calculator as shown in *Figure 19*, which also explained the used parameters. Two suitable springs are found in the catalogue of Amatec^[4], these are shown in *Table 9*. The same calculation can be done for two extension springs, this will give a spring with the same stiffness. But this sub concept is not mentioned any further since the effect is the same, but the assembly of extension springs is much more complicated than the assembly of compression springs.

Table 9: Dimensions springs solution 2 ^[4]

Configuration:	2 parallel (1 top, 1 bottom)		
Name:	Calculator	D21842	C0480-035-1250 S
d (mm)	0.95	0.8	0.89
D (mm)	11.4	11.2	11.3
n (-)	7.2	4	5.2
F_{max} (N)	7.6	11.83	17.38
L_c (mm)	6.84	6.77	10.85
f (mm)	10.04	16.23	20.90
k (N/m)	756.9	730	830
σ (MPa)	257	423	310
L_0 (mm)	16.88	23	31.75

Solution 3: Parallel compression springs

Instead of using just one compression spring on the top and one at the bottom of the moving body, it is also possible to use multiple springs at both sides. The springs all work in parallel, so the total spring stiffness is the sum of the spring stiffness of all the springs. Also, the total spring force is the sum of the spring force of all the springs added. Using this, multiple weaker springs can be used to achieve the same total spring stiffness. The dimension calculator as shown in *Figure 19* is used again to find possible solutions for parallel configurations. Again suitable springs are found in the catalogue of Amatec^[4]. The results are shown in *Table 10*.

Table 10: Dimensions springs solution 3 ^[4]

Configuration	6 parallel (3 top, 3 bottom)		8 parallel (4 top, 4 bottom)		12 parallel (6 top, 6 bottom)	
Name	Calculator	D20780	Calculator	D20790	Calculator	D20790
d (mm)	0.4	0.32	0.32	0.32	0.35	0.32
D (mm)	4	3.2	3.2	3.2	4	3.2
n (-)	16	14	16	20	20	20
F _{max} (N)	2.54	3.16	1.905	3.16	1.27	3.16
L _c (mm)	6.4	4.48	5.12	8.9	7	8.9
f (mm)	10.25	11.21	9.6091	20.4	10.93	20.4
k (N/m)	250	230	198	160	0.12	160
σ (MPa)	404	632	474	316	302	316
L ₀ (mm)	16.65	15.69	14.73	29.3	17.93	29.3

Solution 4: One extension spring in combination with one compression spring

One extension spring is connected on the top side of the moving body, and one compression spring is connected at the bottom of the moving body. This will give another equilibrium position of the moving body. In rest, the moving body will be located at position 0, as far away from the patient as possible.

The influence of this change in rest position on the dissipated power is investigated before considering this concept further. Matlab/Simulink simulations give the average dissipated power for this sub concept. Different spring frequencies are used to see what the influence would be. The results are shown in *Table 11*. From these results, it can be concluded that the change in equilibrium position will cause a higher dissipated power which is undesired.

Table 11: Average dissipated power

	Spring frequency (Hz)	Average P_{diss} (W)
Original rest position (middle)	12.4	1.5299
New rest position (top)	10.0	1.9227
	12.4	1.7972
	15.0	2.0792

Solution 5: Leaf springs

As last solution for the pretension, leaf springs can be used. There is still a lot of freedom in the design of the leaf spring to obtain the desired spring stiffness and low stresses. An advantage of leaf

springs is that the deflection is only half of the stroke: 5mm. Another advantage is that they fulfil the function of linear guidance as well.

A simple calculation of a leaf spring can be made by modelling it as a bending beam. This will give dimensions of the beam which give a rough impression about the sizes to see if it is a realistic solution. The calculations are shown in *Figure 21*. This gives dimensions of the leaf spring in the same order of magnitude as the actuator.

```
syms L b          % Length L, width b of the material, m
F=7.6;           % Spring force, N
k=1520;          % Spring stiffness, N/m
sigma=400*10^6;  % Average stress, Pa
E=210*10^9;      % Elastic modulus, Pa
delta=0.005;     % Deflection, m
h=0.5*10^-3;     % Height of the material, m
[solL,solb]=solve([sigma==6*F*L/(b*h^2),delta==4*F*L^3/(E*b*h^3)], [L,b])
```

Figure 21: Dimension calculator of the leaf spring

5.3.2. Linear guidance

There are five mean solutions for linear guidance of the moving body in the actuator [5]. The advantages and disadvantages of these solutions are explained here. Also, some basic calculations are performed to see if the solution is feasible.

Solution 1: Sliding contact linear motion bearing

A sliding contact linear motion bearing is usually called a plain bearing. Advantages of this type of bearings are the low price, the bearings are very thin, and will be low weight. But plain bearings have one big disadvantage: the friction between the two bearing surfaces will cause wear and temperature rise of the bearing which will decrease the lifetime of the bearing and increase the dissipated power. The friction in a plain bearing is dependent on the sliding contact surface, the load, and the sliding velocity [6]. This application has a high sliding velocity and distance, so the life time of the sliding bearing will be too short.

Solution 2: Rolling element linear motion bearing

There are two types of linear rolling bearings: linear rails, and linear shaft bearings. Both types would be ball bearings. The preference would be the shaft bearing, since the rails are bigger and would add more weight to the actuator. The shaft bearing is located at the centre of the actuator where unused space is left.

Disadvantages of ball bearings are the friction which can cause wear, and the noise the bearing will produce while moving. An advantage is the accuracy of the linear guidance.

To determine if ball bearings have a long enough life time, some calculations are performed. As requirement from the customer, a lifetime of 1217 hours is needed (2 times 20 minutes a day, for 5 years). The method to calculate the life time of a bearing is described in [7], [8] and [9]. This method is for rotation bearings. Some adjustments are made to calculate the lifetime for the linear bearing. These are described in [10] and [11]. This gives an expression for the life time of a linear bearing in hours:

$$L_{10} = \left(\frac{833}{H \cdot n} \right) \left(\frac{C_r}{P} \right)^3 \quad (8)$$

Here is H the travelled distance per oscillation in meter, n is the number of oscillations per minute, C_r the basic dynamic load rating, and P the equivalent dynamic load rating.

Two small bearings are found ^[12] and the life time is calculated. These bearings are: L510X ^[12] and one type that is slightly bigger: L612X ^[12]. The dimensions of the bearings are shown in *Table 12*. Some other properties of the bearings are needed for the calculation:

- $Z = 10$ (number of balls in a row)
- $F_r = mg = 2.5 \text{ N}$ (radial load)
- $F_a = 30 \text{ N}$ (axial load)
- $n = 1200 \text{ osc}$ (oscillations per minute)
- $H = 0.020 \text{ m}$ (distance per oscillation)
- $P = XF_r + YF_a$ (equivalent dynamic load rating, X and Y can be determined using the values above)

Using this and the method as described by Minebea [7] the lifetime for normal use for the L510X and the L612X bearings is calculated. This gave a lifetime of 791 hours and 3668 hours respectively. A life time of 1217 hours is needed in the actuator, so only the L612X bearing can be used for this application.

Table 12: dimensions of the bearings ^[12]

L510X	L612X
d _{inside} = 5 mm	d _{inside} = 6 mm
D _{outside} = 10 mm	D _{outside} = 12 mm
L _{bearing} = 14 mm	L _{bearing} = 18 mm
Ø _{balls} = 1.250 mm	Ø _{balls} = 1.588 mm
C _r = 118 N	C _r = 220 N

Solution 3: Elastic bearing

An elastic bearing would be a leaf spring. This can be applied in two ways. The first option is to make the leaf spring in such a way that it is just big and strong enough to fulfil the function of linear guidance. There is still another spring needed to cause the pretension. The second option is to design a leaf spring that causes the pretension, which automatically will cause linear guidance of the moving body.

The first type is based on designing and controlling degrees of freedom ^[13]. The actuator should only have one degree of freedom left: displacement in the z -direction, the other movements should be constrained. This can be done using wire flexures, which can be approached as very small bars or rods. At least five wire flexures are needed, but mostly 6 are used. The dimensions of these wire flexures depend on the force they have to withstand. This is the radial force: $F_r = mg \approx 2.5 \text{ N}$. The wire flexures should not break when this force is applied, so the buckling force should be larger than the radial force: $F_{buckling} > F_r$. The buckling force is calculated using:

$$F_{buckling} = 4\pi^2 \frac{EI}{L_e^2} \quad (9)$$

With:

$$I_{square\ wire} = \frac{1}{12} t^4 \quad (10)$$

$$I_{round\ wire} = \frac{1}{64} \pi d^4 \quad (11)$$

$$L_e = 2L \quad (12)$$

Using these equations, the combination of the length and thickness of the wire flexure can be calculated. For a length $L = 30\ mm$, the thickness of a square wire flexure is $t = 0.336\ mm$ and for a round wire flexure it would be $d = 0.384\ mm$. This will give the wire flexure a spring constant of $24.849\ N/m$ and the total stiffness of the six wire flexures which account for the linear guidance will be $149.09\ N/m$.

The wire flexures are tested for bucking with an applied force in axial direction. But a force in tangential direction should not cause movement and deflection in this direction, so the stiffness of the wire flexures in this direction is also calculated [14].

$$k_a = \frac{1}{\frac{L}{EA} + \frac{x^2 L}{700EI}} \quad (13)$$

$$k_t = \frac{12EI}{L^3} \quad (14)$$

For a wire flexure of length $L = 30\ mm$, and a square cross section of thickness $t = 0.336\ mm$, this gives an axial stiffness of $165\ kN/m$, and a tangential stiffness of $25\ N/m$.

There are also two ways of connection the leaf springs to the statically body and the moving body which can be considered. This should be attached on two circles. The inner circle can be attached to the statically body or to the moving body, and the outer circle to the static body and the moving body respectively. The connection depends on the dimensions of the other components.

Solution 4: Hydrostatic/aerostatic linear motion bearing

Hydrostatic bearings are like plain bearings, but one big difference is that there is clearance between the moving and stationary body. This is not the case for plain bearings. This clearance is created by a film of oil, water or air between the two bodies and will decrease the friction between the sliding surfaces. Advantages of the hydrostatic bearings are that it can support large loads, the bearings have a very long life time (theoretically infinite) without wear on the surfaces, and high precision and control. Disadvantages of hydrostatic bearings are that they are more expensive, they need maintenance what will increase the costs, are complex in design, and they have high power consumption because of heat generation due to viscous shear in the fluid [15, 16].

Solution 5: Magnetic linear motion bearing

Linear guidance with magnetic linear motion bearings is not investigated any further because the magnetic field of the bearing can interfere with the magnetic field of the actuator. Furthermore, a magnetic bearing uses electrical energy, so more power is needed to accomplish the movement of the moving body which is undesired. A big advantage is that there is no contact between the parts so there will be no friction and noise.

5.3.3. Elimination

Based on the gathered information some solutions will not be suitable for this application. Reasons for this are the price, life time, dissipated power or the complexity.

There were five solutions for the pretension. After some calculations, only the fourth solution (one extension spring and one compression spring) is eliminated since this will cause an unnecessary increase in the dissipated power. The third solution (parallel springs) is also undesired since this is more complex to assemble than just two springs. But if there is a problem with the connection of one spring in a later stage of the design process, this would still be a possible alternative.

From the five solutions for the linear guidance, three solutions are eliminated. These are the sliding bearing, the hydrostatic bearing and the magnetic bearing because of high friction and short life time, price and complexity, and incompatibility respectively. Only rolling bearings and elastic bearing are considered in the further design steps.

5.4. Concepts

From the gathered information and suggested solutions, four concepts are composed which will be investigated in more detail.

- Concept 1: Use custom compression-extension springs in combination with a ball bearing.
- Concept 2: Use compression springs in combination with a ball bearing.
- Concept 3: Use compression springs in combination with an elastic bearing.
- Concept 4: Use a membrane spring with the desired stiffness to fulfil the two functions of pretension and linear guidance with one solution.

The concepts are designed in more detail and drawn in SolidWorks. Furthermore, aspects as the price, size, weight, aesthetics, and safety are investigated. Based on these aspects, the concepts will be ranked and a final concept can be made.

5.4.1. Concept 1: compression-extension springs with ball bearing

This concept with compression-extension springs is complicated to assemble if only one spring is used on the top of the moving body and one at the bottom of the moving body. The spring should be placed in the centre of the back iron, but the ball bearing is also located there. This can be solved in two ways:

- Use more parallel springs at both sides of the moving body. These springs can be located off-centre which will give space for the bearing in the centre.
- Use a linear guidance bearing that is not located in the centre but at the outside of the moving body. This will add more mass on the stationary body.

The second solution will still be complicated to make, so it is chosen to continue with the first option: use more parallel springs. This concept is shown in *Figure 22*. It is chosen to use three springs on top of the moving body and three at the bottom. The properties of the springs are estimated using the spring calculator and gives the dimensions as shown in *Table 8*. This gives an indication about the size of the springs. These springs need to be custom made.

The connection of the springs on the other components will be done with a linear shaft support block as shown in *Figure 20a*. The bearing that is used in the concept is from Micromo ^[12], bearing code L612X. This bearing has the following dimensions: $d_{inside} = 6mm$, $D_{outside} = 12mm$, $B = 18mm$, $\emptyset_{balls} = 1.588mm$, $C_r = 220N$.

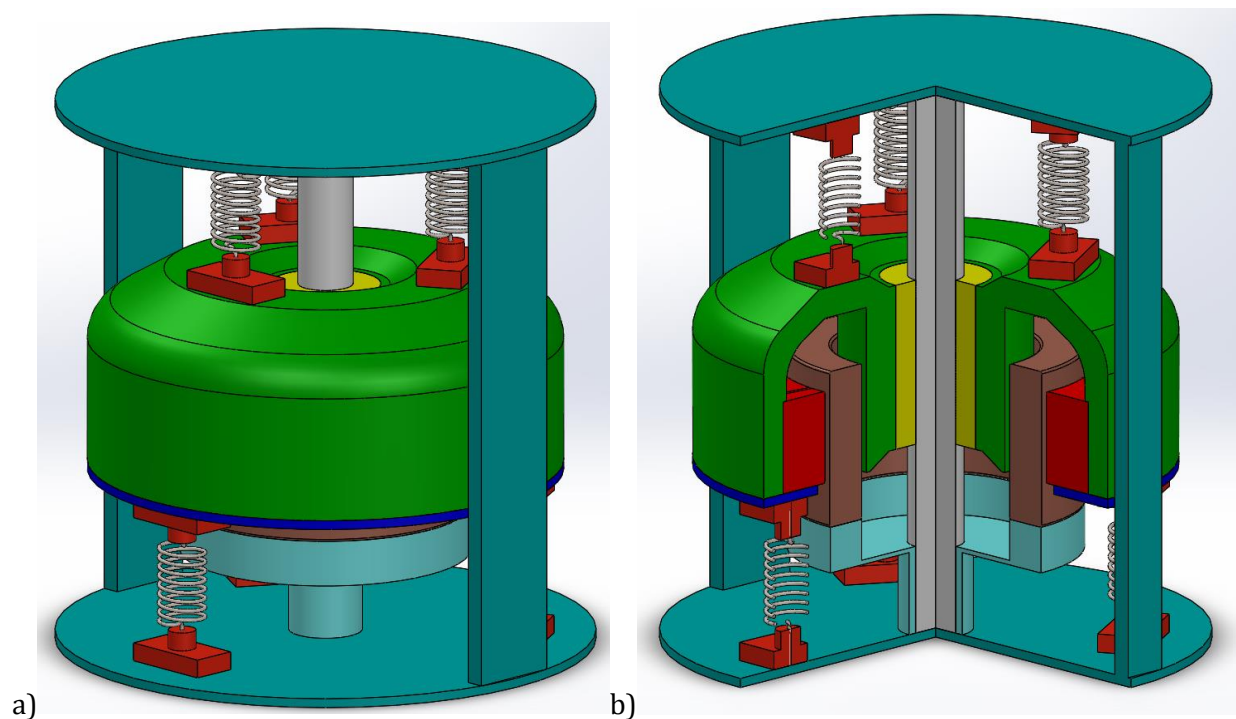


Figure 22: SolidWorks sketch of concept 1, a) complete view, b) cross sectional view, $\frac{3}{4}$ of actuator.
Red: magnets, green: back iron, yellow: bearing, brown: coil, blue: magnet retaining ring.

Advantages of this concept are:

- The springs are in relaxed position (not compressed and not extended) in the equilibrium position of the moving body.

Disadvantages of this concept are:

- The actuator is complex to assemble. The springs are very small and need to be clamped in the linear shaft support block which are also very small and include a lot of small screws. This will make the design complex and hard to assemble.
- Bearings make noise due to friction which might be very unpleasant for the user.

In a later stadium of the design process, some possible improvements are:

- The springs can be relocated and placed next to the back iron instead of on top and underneath it. This will decrease the height of the actuator but increase the diameter of the actuator.
- The use of compression-extension springs allows it to use springs only at one side of the moving body. This will cause a significant decrease in the height of the actuator and decrease the amount of components.

5.4.2. Concept 2: compression springs with ball bearing

Concept 2 is shown in *Figure 23*. The design has two parallel compression springs, one on top of the moving body, and one at the bottom. The compression springs that are used in this design are the D21842 springs, the properties are shown in *Table 9*.

The bearing that is used in the concept is the same as in concept 1, from Micromo ^[12], bearing code L612X. This bearing has the following dimensions: $d_{inside} = 6mm$, $D_{outside} = 12mm$, $B = 18mm$, $\emptyset_{balls} = 1.588mm$, $C_r = 220N$.

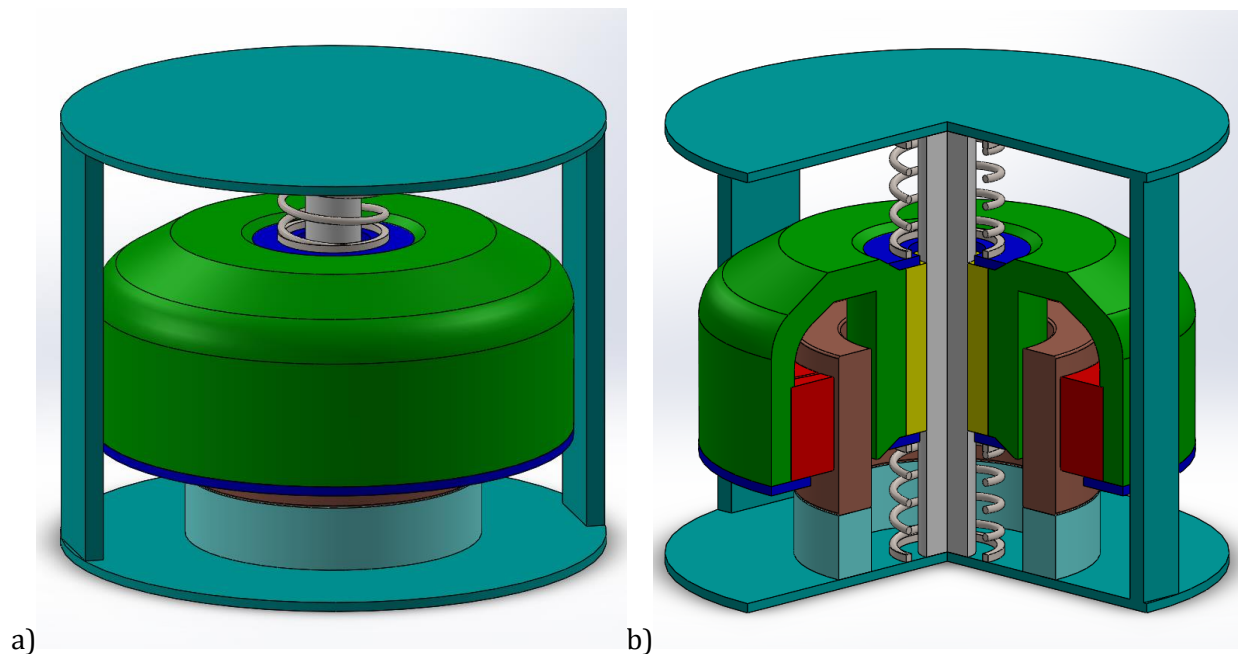


Figure 23: SolidWorks sketch of concept 2, a) complete view, b) cross sectional view, $\frac{3}{4}$ of actuator.
Red: magnets, green: back iron, yellow: bearing, brown: coil, blue: retaining rings.

Advantages of this concept are:

- The actuator is very compact and small.
- The concept has just a few additional components which are not complicated to assemble.

Disadvantages of this concept are:

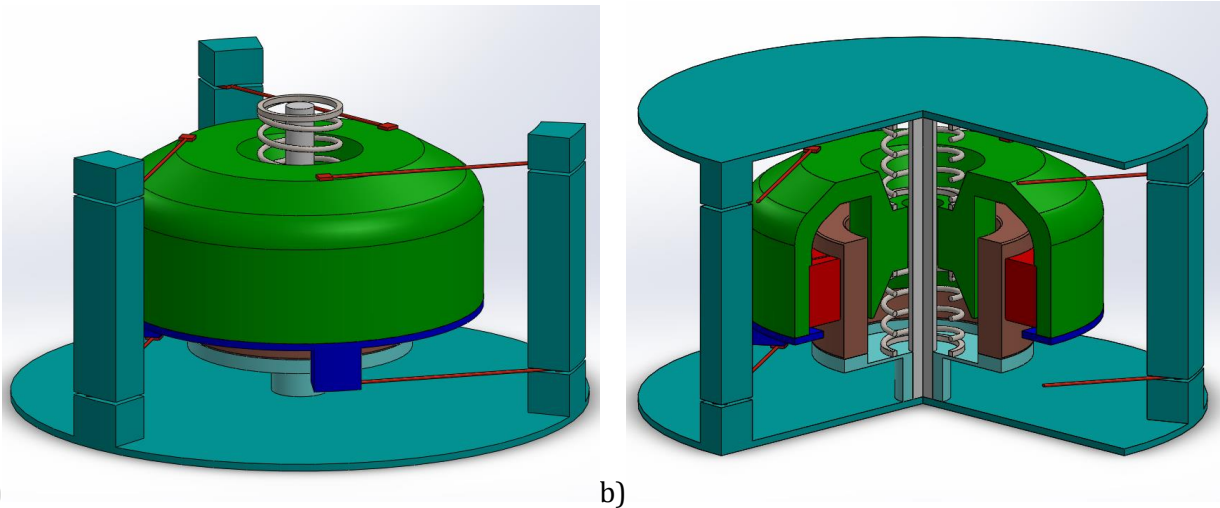
- Bearings make noise due to friction which might be very unpleasant for the user.

5.4.3. Concept 3: compression springs with elastic bearing

This design has two parallel compression springs, one on top of the moving body, and one at the bottom as shown in *Figure 24*. The compression springs that are used in this design are the D21842 springs, just as in concept 2. The properties are shown in *Table 9*.

Wire flexures with a diameter of 0.44 mm and a length of 30 mm are used to ensure the linear guidance of the moving body. The spring constant of one wire flexure follows from buckling calculations and is equal to $k = 45 \text{ N/m}$. So the total stiffness of the wire flexures is $k = 270 \text{ N/m}$. The total stiffness the moving body experience is caused by the helix springs and the wire flexure which are all in parallel. This will give a total stiffness of: $k_{tot} = 2 \cdot k_{helix} + 6 \cdot k_{wire} = 1730 \text{ N/m}$ which gives a spring frequency of 13.24 Hz.

For the wire flexure of length $L = 30 \text{ mm}$, and a square cross section of thickness $t = 0.44 \text{ mm}$, this gives an axial stiffness of 422 kN/m, and a tangential stiffness of 73 N/m.



a) b)
Figure 24: SolidWorks sketch of concept 3, a) complete view (without top), b) cross sectional view, $\frac{3}{4}$ of actuator. Red: magnets, green: back iron, brown: coil, blue: magnet retaining ring, orange/red: wire flexures.

Advantages of this concept are:

- Little noise.
- The actuator is small in height.

Disadvantages of this concept are:

- The wire flexures are very small and thin what will make it almost impossible to make and to assemble. The wire flexures need to be clamped in the stationary body and screwed to the moving body. This will give a lot of small components and a lot of work to assemble.
- The wire flexures need to have a length of 30 mm to be able to withstand the radial force and the stroke. This will give a design with a large diameter of the actuator.

In a later stadium of the design process, some possible improvements are:

- The wire flexures can be made with a square cross section and be bended to decrease the diameter of the actuator.

5.4.4. Concept 4: membrane spring

This concept has six leaf springs, three on top and three at the bottom of the moving body as shown in *Figure 25*. The idea of this design is the same as the wire flexures, but those are made bigger/wider to get the stiffness that is needed for the pretension. The composition of the leaf springs is the same as for the wire flexures which will give the same effect for the linear guidance. Leaf springs with a length of 44.4 mm, width of 6.7 mm, and a thickness of 0.5 mm are used.

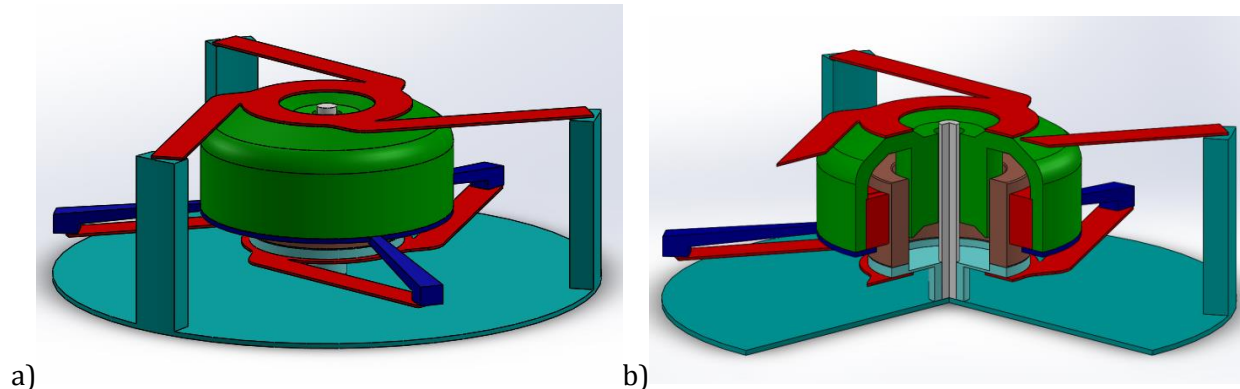


Figure 25: SolidWorks sketch of concept 4, a) complete view, b) cross sectional view, $\frac{3}{4}$ of actuator.
Red: magnets and leaf springs, green: back iron, brown: coil, blue: magnet retaining ring.

Advantages of this concept are:

- The actuator is small in height.
- The concept has just a few components which are not complicated to assemble.
- Little noise.

Disadvantages of this concept are:

- The leaf springs need to have a length of 44.4 mm to be able to withstand the radial force and the stroke. This will give a design with a large diameter of the actuator.

In a later stadium of the design process, some possible improvements are:

- The design of the membrane spring is only based on the calculations of a leaf spring using the deflection formulas. The design and the diameter of the membrane spring can be optimised to decrease the total diameter of the actuator.
- The radius of the inner circle of attachment of the leaf springs can be made smaller. Some extra material with a small radius can be added on top of the back iron to attach the leaf springs to. The same can be done with the bottom of the coil. If the inner circle is smaller, the outer circle can also be made smaller what will result in an actuator with a smaller diameter.

5.4.5. Summary of the concepts

Some general information about the four concepts is summarized in *Table 14*. The masses and dimensions shown here are estimated after optimization of the concepts. It can be seen that the mass is too high for all four concepts. In all concepts there is a possibility to decrease mass by adjusting the coil carrier, the shaft and the stand. The diameter of the actuator in concept 3 and 4 can also be decreased by optimization of the leaf springs and wire flexures. This will also give a decrease in mass.

Table 14: Summary of properties of the four concepts

Properties	Concept 1	Concept 2	Concept 3	Concept 4
Height h (mm)	65	55	50	45
Diameter D (mm)	60	60	70	75
Total mass (g)	340	320	360	370
Mass moving body (g)	220	215	210	225
# elements pretension	18	2	2	2
# elements linear guidance	1	1	6	2

The analysis of the mass of all the separate parts is added in *Appendix C*. These masses are based on parts made of steel AISI 1020 in SolidWorks with a density of 7900 kg/m³. Only the springs, magnets and coil have different specified materials. These are respectively stainless steel (ferritic) with a density of 7800 kg/m³, NdFeB 48 with a density of 7500 kg/m³, and copper with a density of 6370 kg/m³. More mass can be saved by using different materials than steel where possible.

5.5. Selection of the concepts

A list of concept selection criteria is made to be able to compare the four concepts and select the final concept. Each criterion got a weighing factor based on the importance of this particular criterion. All concepts are ranked for every criterion, this is multiplied with the weighing factor and gives an end score for all four concepts. The ranking is based on the drawn concept and the optimization opportunities on this concept. For example the size of concept 3 and 4 can be reduced a lot, so the concepts are ranked based on this estimated achievable diameter. The criteria and ranking is shown in *Table 15* below ^[17].

Table 15: Concept selection matrix, Pugh Matrix (--, -, 0, +, ++)

Criteria	Weight	Concept 1	Concept 2	Concept 3	Concept 4
Functionality	3	+	+	+	+
Total weight	3	0	+	-	-
Price	3	-	+	-	0
Size	2	+	++	0	+
Durability/life time	2	0	0	+	+
Complexity of the design	2	-	+	-	0
Aesthetics	1	--	++	--	++
Noise	1	-	-	+	+
Assemble time	1	--	+	--	0
Total	18	-5	17	-6	7

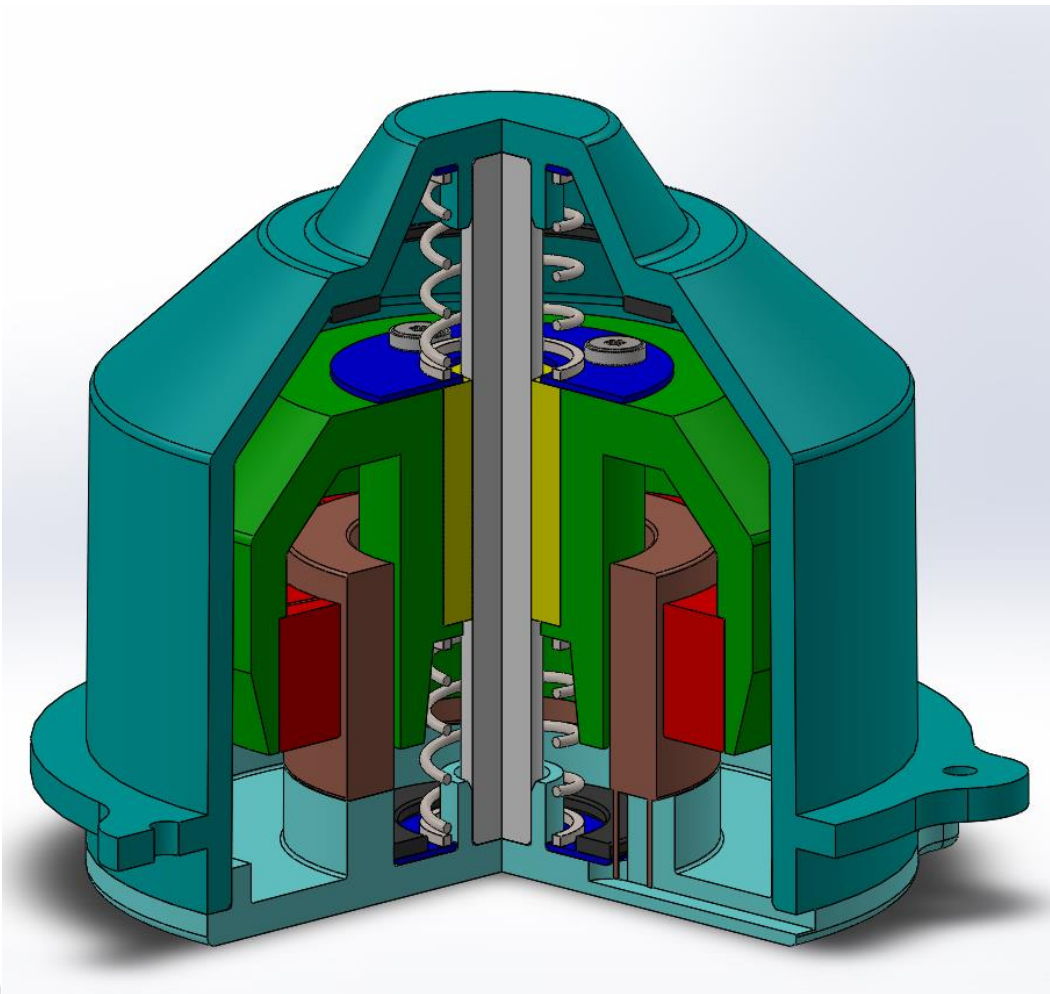
Concept 2 has the highest score and will be used as basis for the final design of the actuator. Concept 4 will be kept as back up in case that concept 2 is not feasible.

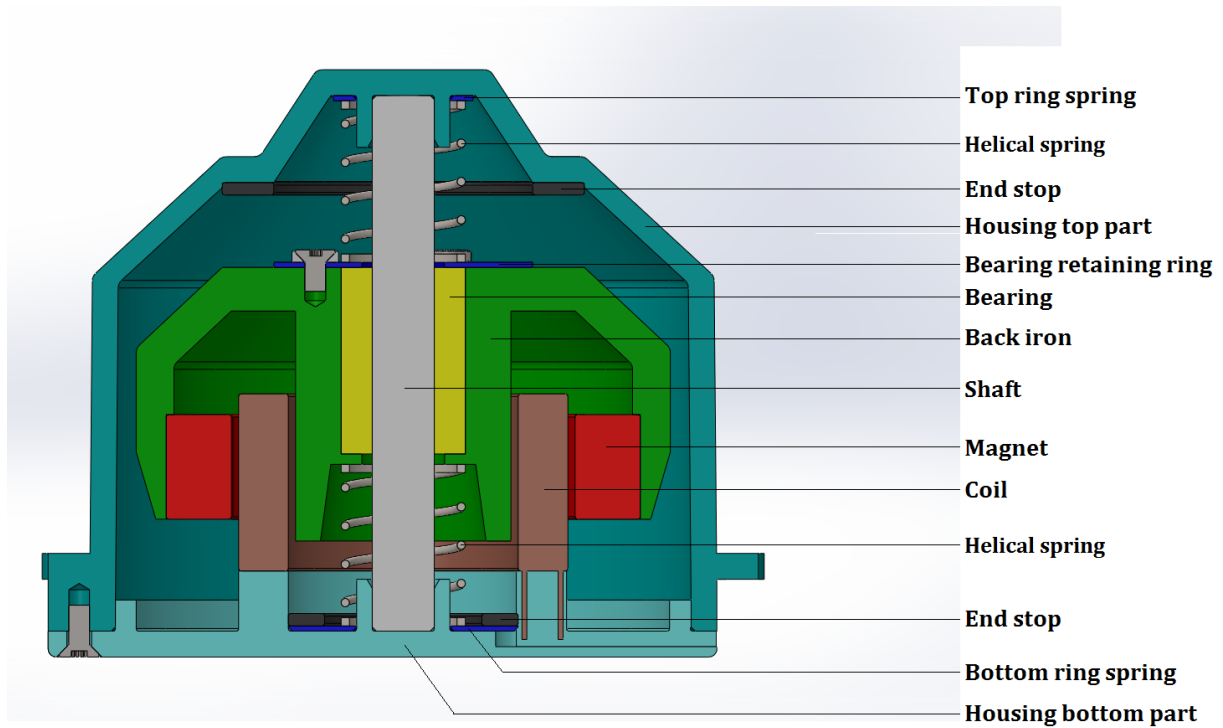
5.6. Final concept

The way concept 2 is drawn in the previous section gives a rough idea of what the actuator should look like. Some aspects can be optimised and some parts are not included in the design yet. Additional calculations and mass optimizations are performed and some additional parts are designed. Another important thing to keep in mind during the design is that the actuator should be designed for mass production of 16.000 pieces a year. This will influence the production processes and the detailed design.

5.6.1. Total overview

A final design of the actuator is made and shown in *Figure 26* and *Figure 27*. The optimization and adjustments, and design of the details are explained later in this section. The total mass of the actuator is 330 grams from which the moving body weighs 220 grams. The detailed distribution of the mass is added in *Appendix C*. The total height of the actuator is 56.7 mm and the diameter of the actuator is 68.6 mm.





b)

Figure 26: Final design of the actuator, a) cross section, $\frac{3}{4}$ of actuator, b) cross section $\frac{1}{2}$ of actuator

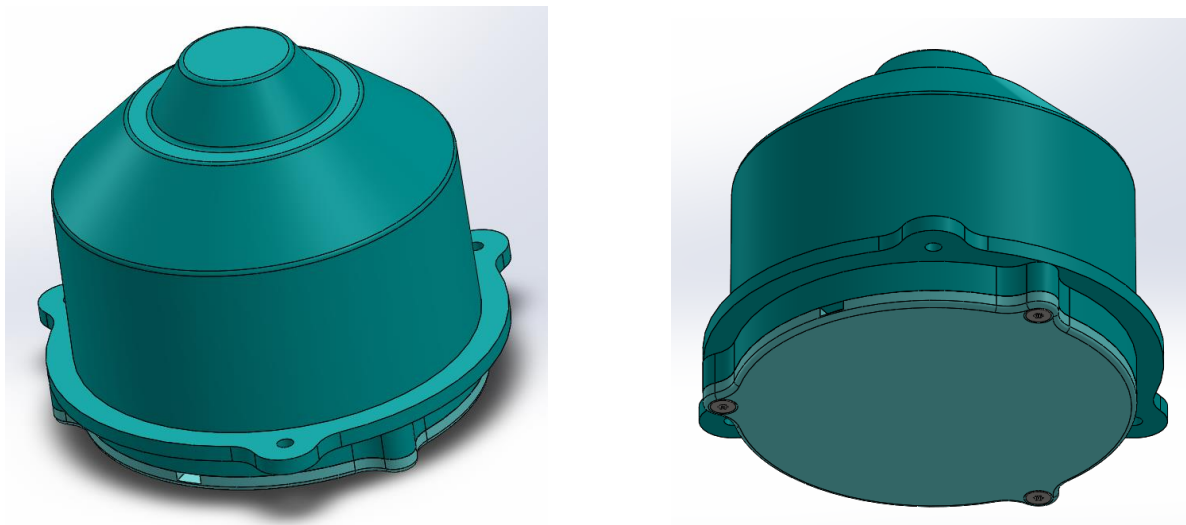


Figure 27: Outside view of the actuator

5.6.2. Optimization and adjustments

Holding force magnet

The holding force between the magnet and the back iron can be calculated using FEMM with the function 'Force via weighted stress tensor'. This gives a holding force of 36.9 N of all the magnets together. The holding force for one magnet will be 4.6 N. To detach this magnet, an acceleration of 64g should be applied on the particular magnet. From this calculation it can be concluded that the

magnets will not detach and do not need support to stay in position. So the support ring at the bottom of the magnets is not necessary and is removed in the final design. The shape of the back iron where the ring was attached is optimised as well.

A small edge is made in the back iron to place the magnets against. This edge is 0.5mm wide. Increasing the width of this edge will increase the holding force of the magnets. If this edge is 0.75mm wide, an acceleration of 72g is needed to detach the magnet. Based on this, the width of the edge will be increased to 0.75mm.

Length of the pretension springs

The springs (spring D21842, properties are shown in *Table 9*) are placed in the actuator in pretension. The Stiffness of this spring is 730 N/m and the average stress is 420 MPa. The closed length of the springs is 6.77mm and the stroke is 16.23mm. A displacement of 5mm is necessary; using a safety factor gives a needed displacement of 8 mm. This safety factor is based on the deflection of the springs cause by gravity: $F_z = k \cdot \delta$ which can already give a deflection of 1.6 mm.

So the spring needs to have a length of $L_0 + 8 \approx 14.8$ mm in the equilibrium position.

5.6.3. Detailed design

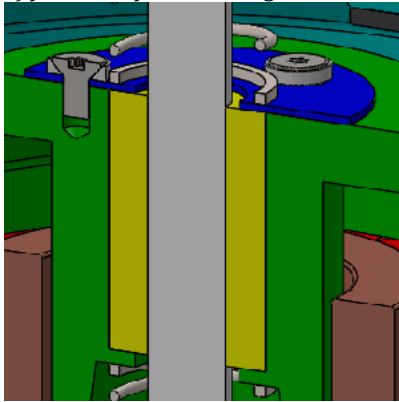
There are a couple other aspects on the design of the actuator that need to be looked into:

- The fixation of the bearing and creating a flat contact surface for the springs on the moving body
- The connection between the shaft and the housing
- The connection between the coil carrier and the housing
- The design of the end stops
- The design of the housing

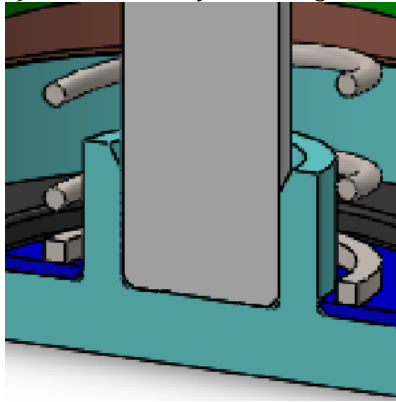
Design concepts are created and added in *Appendix D* for all aspects including advantages and disadvantages. Based on these advantages and disadvantages, an estimation of the feasibility, the price and the ability to combine solutions from different aspect, a selection is made. The selected design solutions are shown in detail in *Figure 28*. To fixate the bearing, it is chosen to press it against an edge of the back iron at the bottom, and to fix it with a ring on top of the back iron. This will also create a flat contact surface for the springs on both sides of the back iron. The housing is made out of two parts put together with screws. The top part contains the top and the sides of the housing and can be made by injection molding. The design is adjusted to get the part out of the mold. The second part is the bottom of the housing with integrated coil carrier. The shaft is clamed in the housing with a ring that encloses it. The rubber end stops are glues to the top and bottom of the housing.

Furthermore, some rings are added to distribute the load applied by the springs on the housing over a bigger surface of the housing. Also three screw holes are added on the top part of the housing to be able to connect the actuator to the vest. A coil wire channel is left in the bottom part to lead the wire out of the actuator.

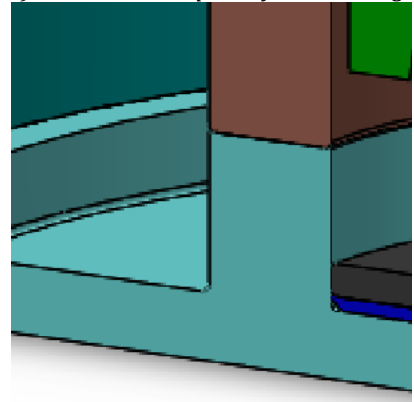
a) fixation of the bearing



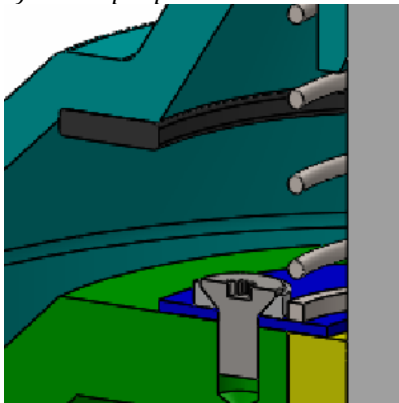
b) connection shaft – housing



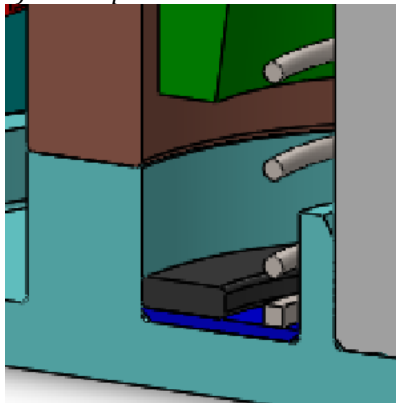
c) coil carrier as part of the housing



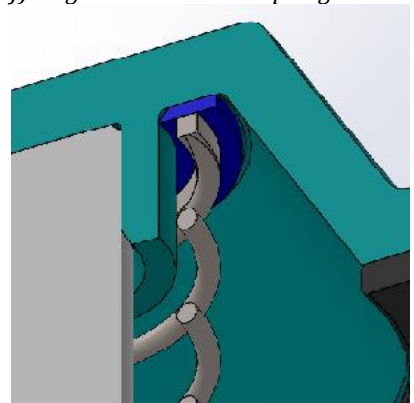
d) end stop top



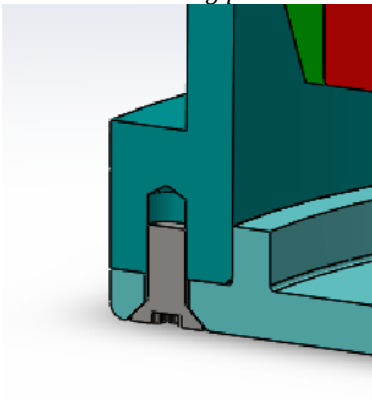
e) end stop bottom



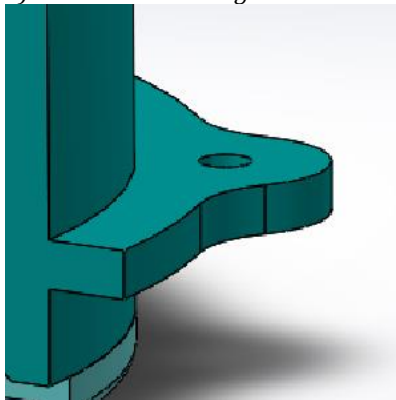
f) ring underneath the spring



g) connection housing parts



h) connection housing – vest



i) coil cable channel

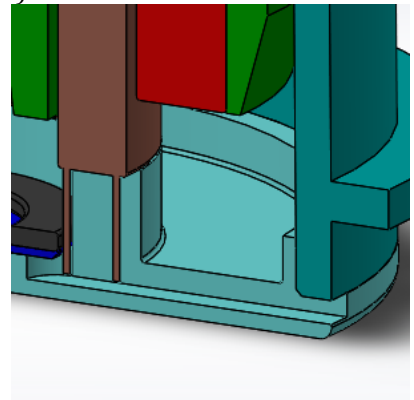


Figure 28: Detailed view of design aspects

All parts of the actuator need to be assembled in the correct order. First, the magnets and the bearing are placed in the back iron. The bearing is fixed with the ring and screws to the back iron. Second, the top end stop, the ring underneath the spring, and the shaft are attached to the top part of the housing. Third, the coil, the ring underneath the spring and the bottom end stop are attached to the bottom part of the housing. As last step, the three created subassemblies are assembled starting with the top part of the housing. Hold the top part of the housing upside down and put the

first helical spring, the back iron, the second helical spring, and the bottom part of the housing over the shaft. Fixate everything by screwing the top part and the bottom part of the housing together.

5.6.4. Moving actuator

Figure 29 shows the actuator in different configurations. During normal movement of the actuator, it has a safety tolerance on all sides of 2mm. Furthermore is it shown that when the moving body hits the end stop, it only makes contact with the end stop, no other parts touch the housing.

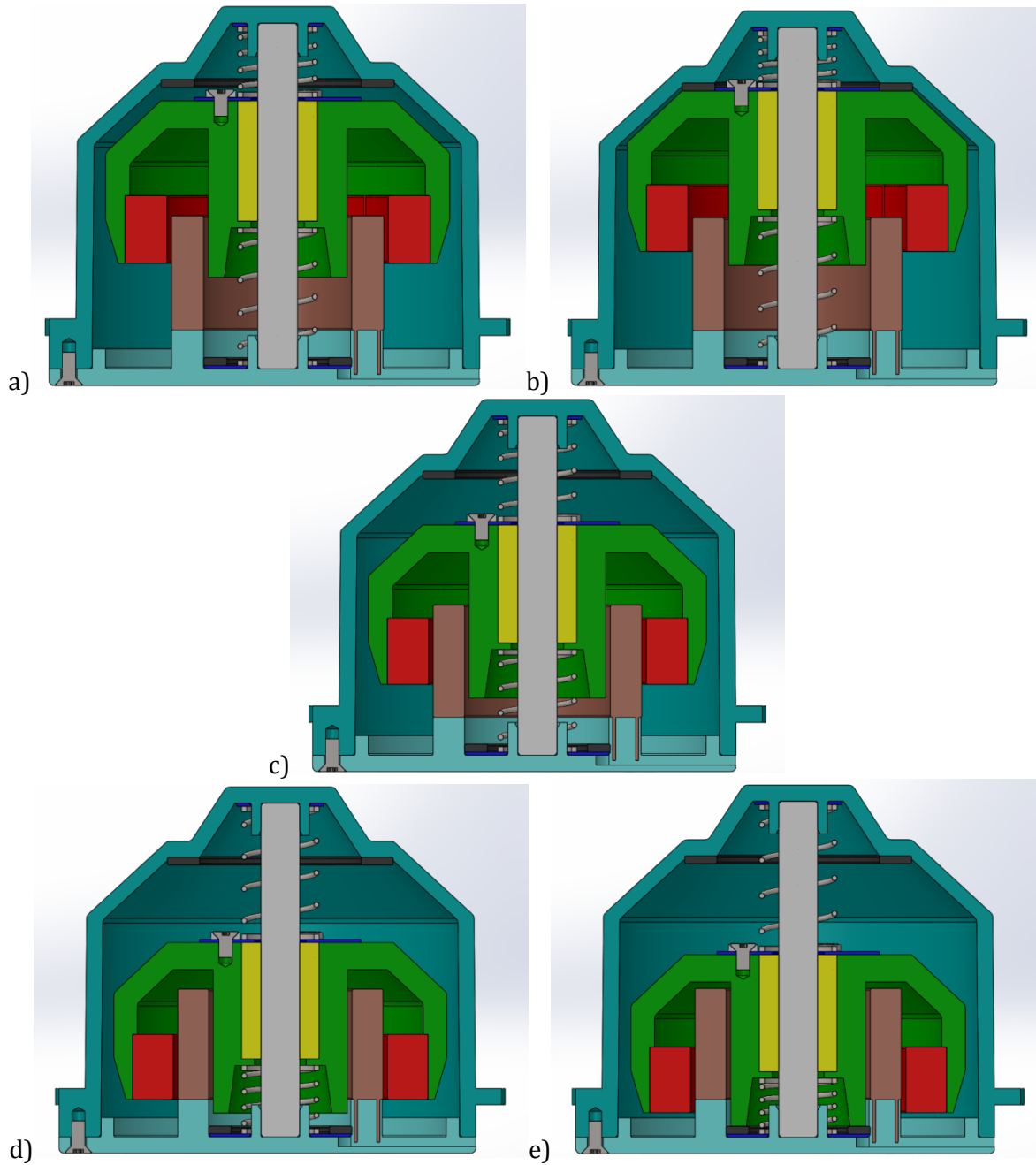


Figure 29: The actuator on different configurations a) 5mm stroke up, b) 7mm, end stop up, c) equilibrium position, d) 5 mm stroke down, e) 7mm, end stop down

Conclusions

From the first part of the research, the sensitivity analysis and the optimisation of the waveform, some conclusions can be drawn. First of all, the discretisation problem can be solved using a look-up table which contains the deviations from the simulated therapy force with respect to the set therapy force for every possible setting. In the model, the simulated therapy force is corrected for this deviation to create a signal without deviations.

The sensitivity analysis showed the influence of variations in the mass, the spring stiffness, the coil resistance, the motor constant, and the coil inductance on the therapy force. It also showed that the therapy force is influenced mostly by deviations in the mass, and in variations in the coil resistance. Using some test results, tolerances for the parameters are set to keep the deviations in therapy force low. This gave some optimisation and improvements on the control system of the actuator which decreased the dissipated power and improved the accuracy.

The results from the sensitivity analysis are compared to the results of an analytical solution. The Taylor series expansion with respect to the five parameters showed that the influence of the mass on the therapy force is the most important and the influence of the coil inductance the smallest. This is similar to the result of the sensitivity analysis.

As third, a waveform optimisation is performed. Different waveforms are compared for high and for low therapy frequencies. This showed that the optimised original waveform is the best. This gives a low dissipated power and a high impulse while the moving body stays within the boundaries.

In the second part of the research, a redesign of the actuator is made. This design is low weight and compact. The goal of the redesign is achieved: the total mass of the new actuator is 331 grams which is less than the desired 350 grams. The mass of the moving body is 220 grams. The total height of the actuator is 56.7 mm and the diameter of the actuator is 68.6 mm. A leaf spring is used in the original design to responsible for the pretension and the linear guidance. In the redesign, this is replaced by helical compression springs and a ball bearing. The dissipated power of the new actuator stays below the 3W as desired.

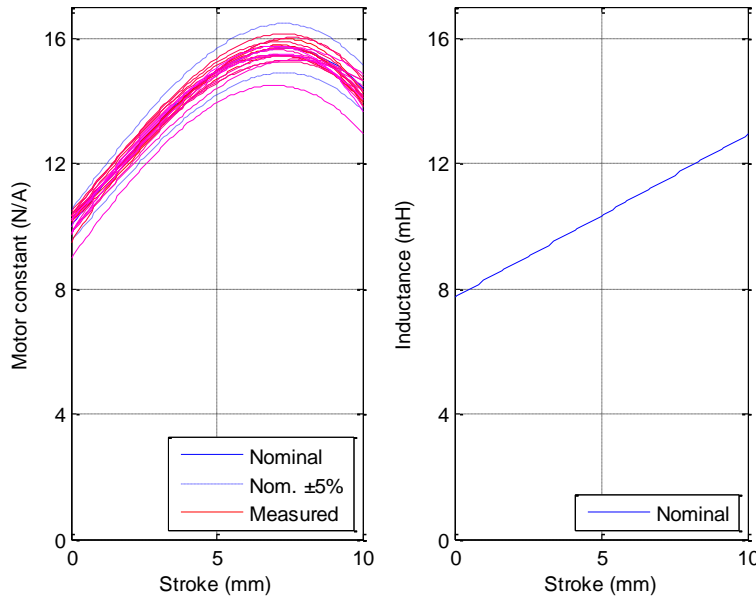
So the redesign fulfils all requirements and would be a good alternative actuator for the vest for patients with cystic fibrosis.

References

- [1] D. Tjepkema, R. Hesselink, 0398-14-001 *confidential name* CDD v1.0.docx
- [2] Amar M.R.S., Estimation of Mechanical Properties of Soft Tissue Subjected to Dynamic Impact, University of Nebraska at Lincoln, 2010, p41-42, URL:
<http://digitalcommons.unl.edu/cgi/viewcontent.cgi?article=1009&context=imsediss>
- [3] Werktuigbouw&tribologie, Calculator for round wire helical springs, URL:
<http://www.werktuigbouw.nl/sub17.htm>
- [4] Amatec technische veren B.V., URL: <http://www.amatec.nl/>
- [5] NSK Ltd., Precision Machinery & parts, URL:
http://www.nskamericas.com/cps/rde/dtr/na_en/na_literature_Linear/Linear_Guide_Tutorial.pdf
- [6] Werktuigbouw&tribologie, Journal bearing service life, URL: http://www.tribology-abc.com/calculators/e4_4.htm
- [7] Minebea, Ball Bearing Load Ratings and Life Calculations, URL:
<http://www.nmbtc.com/bearings/engineering/load-life/>
- [8] AST bearings and related products&services, Technical information, Life and Load Ratings – Radial ball bearings, URL: <http://www.astbearings.com/assets/files/Technical-Information-Sheet--Radial-Ball-Bearings-Life-and-Load-Ratings--ENB-04-0637.pdf>
- [9] Schaeffler, Medias professional – product catalogue, Load carrying capacity and life, URL:
http://medias.schaeffler.de/medias/en!hp.tg.cat/tg_wf*ST4_307653387
- [10] Misumi, Calculation of Life Spam of Linear Ball Bushings, URL: http://us.misumi-ec.com/pdf/fa/2009/inch_p075.pdf
- [11] Thomson Linear motion optimised, Selecting and applying rolling element linear bearing and guides, Page 5, URL:
http://www.thomsonlinear.com/downloads/articles/Selecting_Applying_Rolling_Element_Linear_Bearings_Guides_tae.pdf
- [12] Micromo, Microlinea, linear bearings catalogue, URL: <http://www.micromo.com/media/pdfs/mps-microsystems-microlinea-linear-bearings-l.pdf>
- [13] Herman Soemers, Design principles for precision mechanisms, 2010
- [14] Janssen Precision Engineering, Flexure engineering fundamental – rod spring, URL:
<http://www.janssenprecisionengineering.com/page/flexure-engineering-fundamental-rod-spring/>
- [15] HIS Engineering360, Hydrostatic and hydrodynamic bearings information, URL:
http://www.globalspec.com/learnmore/mechanical_components/bearings_bushings/hydrostatic_hydrodynamic_bearings
- [16] MachineBuilder.net, Hydrostatic linear bearings are simple to install, URL:
<http://www.machinebuilding.net/p/p1741.htm>
- [17] Stuart Burge Dr, The systems Engineering Tool Box, Pugh Matrix (PM), URL:
<http://www.burghugheswalsh.co.uk/uploaded/1/documents/pugh-matrix-v1.1.pdf>

Appendices

Appendix A: results measurements prototypes



R (Ohm)	wr (Hz)	km.a	km.b	km.c	km.d	
3.84 (0.05)	12.700 (0.00)	-0.0093631	0.0283981	1.0505	10.14973	dev001HF
3.83 (0.05)	12.650 (0.07)	-0.0148391	0.1127795	0.7625	10.16389	dev002HF
3.89 (0.06)	12.400 (0.00)	-0.0095792	0.0374877	0.9680	10.10192	dev003
3.87 (0.05)	12.400 (0.00)	-0.0130746	0.0809887	0.8519	10.32113	dev004
3.91 (0.06)	12.300 (0.00)	-0.0047659	-0.0537115	1.4645	9.47078	dev005
3.84 (0.05)	12.400 (0.00)	-0.0079896	0.0005584	1.1792	10.22047	dev006
3.85 (0.06)	12.350 (0.07)	-0.0091496	0.0250599	1.0849	10.44328	dev007
3.85 (0.05)	12.550 (0.07)	-0.0076821	-0.0003201	1.1705	10.33756	dev007HF
3.84 (0.04)	12.350 (0.07)	-0.0043851	-0.0449585	1.2678	10.29445	dev008
3.83 (0.04)	12.750 (0.07)	-0.0119300	0.0818119	0.8124	10.35374	dev008HF
3.89 (0.06)	12.650 (0.07)	-0.0057085	-0.0104641	1.0725	10.20727	dev011HF
3.89 (0.05)	12.350 (0.07)	-0.0025829	-0.0558315	1.3047	9.75827	dev012
3.88 (0.05)	12.750 (0.07)	-0.0113131	0.0559840	1.0067	9.78141	dev012HF
3.80 (0.05)	12.350 (0.07)	-0.0098247	0.0308164	1.0269	10.29276	dev014
3.84 (0.05)	12.300 (0.00)	-0.0082479	0.0272346	0.9574	10.22320	dev015
3.89 (0.07)	12.300 (0.00)	-0.0067006	0.0107209	1.0252	9.83250	dev017
3.86 (0.05)	12.300 (0.00)	-0.0056671	-0.0337101	1.3034	8.96090	dev018
3.88 (0.05)	12.300 (0.00)	-0.0034342	-0.0498449	1.3285	9.98103	dev019
3.94 (0.05)	12.300 (0.00)	-0.0068686	-0.0135637	1.2488	9.76683	dev020
3.89 (0.05)	12.350 (0.07)	-0.0118242	0.0523295	1.0069	10.18499	dev021

The used Matlab code to find the mean value, standard deviation and the tolerance:

```
%Calculation of mean, standard deviation (using deviation 1% for the mass)
mean_m=0.387; Mm_var=0.01;
R=[3.84 3.83 3.89 3.87 3.91 3.84 3.85 3.85 3.84 3.83 3.89 3.89 3.88 3.80 3.84 3.89
3.86 3.88 3.94 3.89]; %Values from data
omega=[12.70 12.65 12.40 12.40 12.30 12.40 12.35 12.55 12.35 12.75 12.65 12.35
12.75 12.35 12.30 12.30 12.30 12.30 12.30 12.35]; %Values from data
K=mean_m*(1+Mm_var)*(2*pi*omega).^2;

std_R=std(R); std_omega=std(omega); std_K=std(K);
mean_R=mean(R); mean_omega=mean(omega); mean_K=mean(K);
tolerance_R=3*std_R/mean_R
tolerance_omega=3*std_omega/mean_omega
tolerance_K=3*std_K/mean_K
```

Appendix B: derivation transfer function

There are three main equations necessary to derive the transfer function. These are the equation of motion, a relation between the actuator force, the motor constant and the current, and an equation for the voltage.

$$U = IR - \dot{x}k_m + L_m \frac{dI}{dt} \rightarrow I = \frac{U + k_m s x}{R + L_m s} \left\{ \begin{array}{l} F_{act} = k_m \frac{U + k_m s x}{R + L_m s} \\ F_{act} = k_m I \end{array} \right.$$

$$\left. \begin{array}{l} F_{act} = -kx - m\ddot{x} = -(k + ms^2)x \\ F_{act} = k_m I \end{array} \right\} \rightarrow \left(\frac{k_m}{R + L_m s} \right) U = - \left(ms^2 + k + \frac{k_m^2 s}{R + L_m s} \right) x$$

Multiply both sides by ms^2 :

$$\left(\frac{k_m}{R + L_m s} \right) ms^2 U = - \left(ms^2 + k + \frac{k_m^2 s}{R + L_m s} \right) ms^2 x$$

On the right had side we can recognise: $ms^2 x = F_{th}$

$$\left(\frac{k_m}{R + L_m s} \right) ms^2 U = - \left(ms^2 + k + \frac{k_m^2 s}{R + L_m s} \right) F_{th}$$

This will give the transfer function:

$$\frac{F_{th}}{U}(s) = \frac{k_m ms^2}{(R + L_m s)(ms^2 + k) + k_m^2 s}$$

Appendix C: Mass analysis of the concepts and final design

The masses shown here are the masses as calculated by SolidWorks of the parts as they are drawn in the concepts. No mass or dimension optimization is performed.

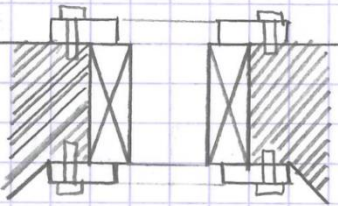
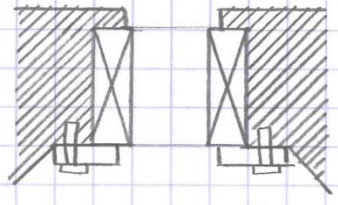
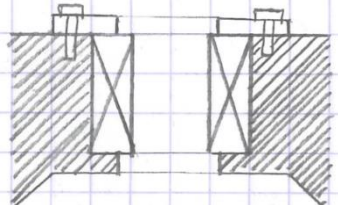
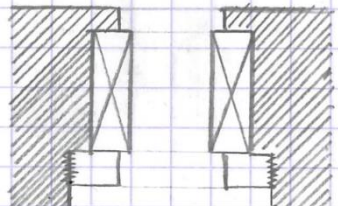
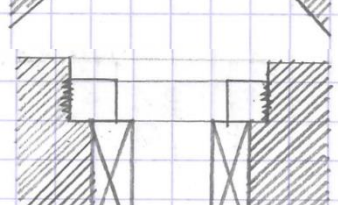
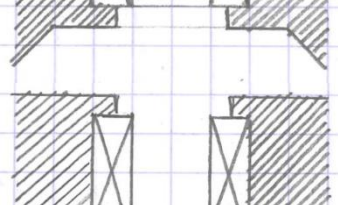
Part	Material in SW	Density (kg/m ³)	mass (g)			
			Concept 1	Concept 2	Concept 3	Concept 4
Coil	Copper coil	6370	44.32	44.32	44.32	44.32
Back iron	AISI 1020	7900	134.97	134.97	136.58	146.87
Ring bottom	AISI 1020	7900	8.74	6.59	11.55	13.41
8 magnets	Magnet NdFeB48	7500	59.12	59.12	59.12	59.12
Shaft	AISI 1020	7900	13.06	10.10	4.09	3.49
Coil carrier	AISI 1020	7900	18.60	22.19	9.69	9.84
Stand	AISI 1020	7900	61.09	56.9	128.22	117.78
Springs (helix)	Stainless steel	7800	0.84	1.74	1.74	
Wire flexure/leaf spring	Stainless steel	7800			0.36	13.20
Springs connections	AISI 1020	7900	10.80			
Bearing	AISI 1020	7900	12.06	12.06		
Fixation rings bearing	AISI 1020	7900		2.28		
Total mass:			363.58	350.26	389.83	408.04
Mass moving body:			220.71	215.89	208.30	226.00

The masses shown below are the masses as calculated by SolidWorks of the parts as they are drawn in the final design.

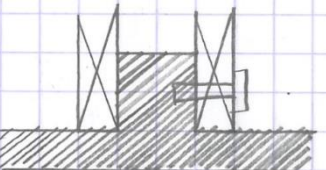
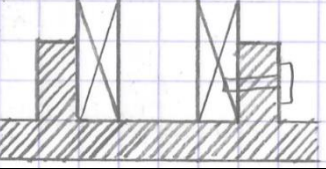
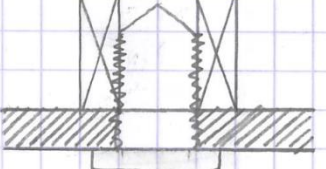
Part	Material in SW	Density (kg/m ³)	Amount	Mass (g)	Total mass (g)
Coil	copper coil	6370	1	44.34	44.34
Back iron	AISI 1020	7900	1	150.65	150.65
Magnets	Magnet NdFeB48	7500	8	7.39	59.12
Shaft	AISI 1020	7900	1	11.53	11.53
Housing bottom	POM Acetal copolymer	1390	1	14.74	14.74
Housing top	POM Acetal copolymer	1390	1	36.58	36.58
Screw housing	AISI 1020	7900	3	0.16	0.48
Bearing	-	-	1	7.00	7.00
Retaining ring bearing	AISI 1020	7900	1	1.70	1.70
Retaining ring screw	AISI 1020	7900	3	0.14	0.42
Retaining ring screwring	AISI 1020	7900	3	0.07	0.21
Spring	Stainless steel (ferritic)	7800	2	0.87	1.74
Ring spring top	AISI 1020	7900	1	0.30	0.30
Ring spring bottom	AISI 1020	7900	1	1.22	1.22
End stop top	BUTYL	1159	1	0.65	0.65
End stop bottom	BUTYL	1159	1	0.28	0.28
Total mass:					330.95
Mass moving body:					219.97

Appendix D: Other design aspects concepts

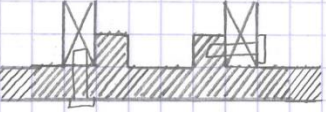
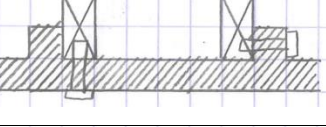
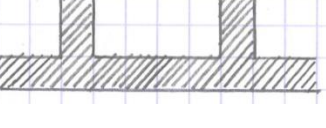
Connection of the bearing to the back iron:

Concepts	Description – Pros – Cons
	Attach a ring on top and at the bottom of the bearing and fix it with screws to the back iron
	Pros: simple design of the additional parts
	Cons: screws make the design big, higher assemble time due to screwing, not enough space at the bottom due to the spring and back iron.
	Press the bearing against an edge on top of the back iron to fix it on one side. Fix the bottom side with a ring and screws in the back iron.
	Pros: simple design of the additional parts
	Cons: screws make the design big, not enough space at the bottom due to the spring and back iron, longer assemble time
	Press the bearing against an edge at the bottom of the back iron to fix it on one side. Fix the top side with a ring and screws in the back iron.
	Pros: simple design of the additional parts
	Cons: Screws make the design big, longer assemble time
	Press the bearing against an edge at the top of the back iron to fix it on one side. Fix the bottom side with a ring with screw thread/rifling.
	Pros: simple to assemble, just one additional part, a good surface for the spring is present on both sides.
	Cons: complicated component, needs to be big enough to contain rifling
	Press the bearing against an edge at the bottom of the back iron to fix it on one side. Fix the top side with a ring with screw thread/rifling.
	Pros: simple to assemble, just one additional part, a good surface for the spring is present on both sides.
	Cons: complicated component, needs to be big enough to contain rifling, additional material needed on top of the back iron to attach the ring
	Press the bearing against an edge on top of the back iron to fix it on one side. Fix the bottom side with a retaining ring in the housing.
	Pros: retaining ring is a standard part, simple to assemble
	Cons: on one side a surface for the spring is missing so an additional ring needs to be added. In this case, this ring can also be located in such a way that it immediately fixates the bearing.

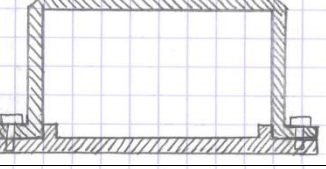
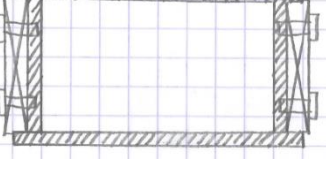
Connection of the shaft to the housing:

Concepts	Description - Pros - Cons
	Add a support plug that fits inside the shaft (can be fixated with a screw)
	Pros: small, does not interfere with the spring
	Cons: high tolerances needing in height and in width
	Add a support ring that fits around the shaft (can be fixated with a screw)
	Pros: more contact area and strong
	Cons: high tolerances needing in height and in width
	Add screw thread/rifling on the inside of the shaft and attach it with a screw from the bottom/top.
	Pros: does not interfere with the spring
	Cons: complicated to align, more production/assemble time

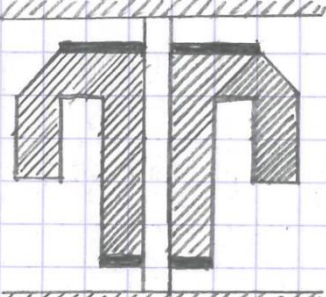
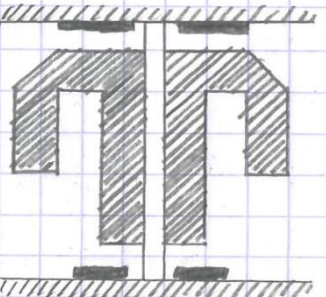
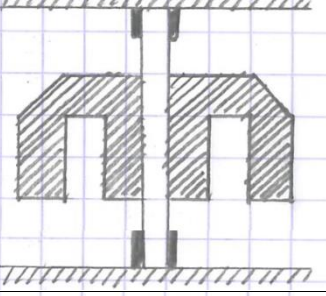
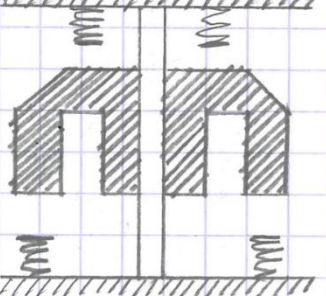
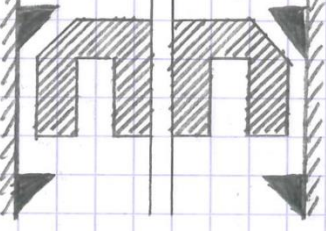
Connection of the coil carrier to the housing:

Concepts	Description - Pros - Cons
	Add a support ring on the ground plate of the housing that fits inside the coil carrier (can be fixated with a screw/glue)
	Pros: can be combined with the end stop, easy to assemble
	Cons: screw can interfere with the spring
	Add a support ring on the ground plate of the housing that fits around the coil carrier (can be fixated with a screw/glue)
	Pros: easy to assemble and produce
	Cons: additional time to screw/glue the parts together
	Combine the ground plate of the housing with the coil carrier. Add a ring on the ground plate which has the exact size of the desired coil carrier.
	Pros: no additional components needed
	Cons: makes the design of the housing a little more complicated

Design of the housing:

Concepts	Description - Pros - Cons
	Combine the function of the stand with the housing. Use a ground plate and a cap and close it with screws.
	Pros: low weight, simple assembly
	Cons: thick wall needed because the housing will be mechanically loaded
	Use only a cylinder to close the sides, needed if the stand is not combined with the housing. Screw this cylinder in the vertical bar of the stand and then screw the top of the stand on top of the vertical bars.
	Pros: thin wall
	Cons: more work and complicated to assemble

Design of the end stops:

Concepts	Description – Pros – Cons
	Use a circular rubber ring with a radius bigger than the springs as end stop. Attach this at the right distance to the back iron. The inner ring of the back iron can be elongated to get the right distance.
	Pros: the additional mass is added to the moving body. Cons: -
	Use a circular rubber ring with a radius bigger than the springs as end stop. Attach this at the right distance to the housing.
	Pros: the rubber ring does not move along with the oscillations Cons: the additional mass is added to the static part.
	Use a circular rubber ring with a radius smaller than the springs as end stop. Attach this to the shaft and the housing.
	Pros: small, adds the minimal amount of weight Cons: there is not much space between the shaft and the springs, so the width of the rubber ring needs to be very small.
	Add another spring attached to the housing with a high stiffness that will only make contact with the moving body if the stroke is getting to big.
	Pros: spring does not need to be custom made Cons: Complicated to assemble, additional assembly parts are needed, impact force
	Add a rubber damping block on the cylinder of the housing or the vertical bars of the stand
	Pros: little extra material is added Cons: complicated to attach to the housing